Published in final edited form as:

Brain Struct Funct. 2016 May ; 221(4): 1809–1831. doi:10.1007/s00429-015-1005-z.

The RNA-binding protein Celf6 is highly expressed in diencephalic nuclei and neuromodulatory cell populations of the mouse brain

Susan E. Maloney[1,2], **Eakta Khangura**[1,2], and **Joseph D. Dougherty**[1,2]

[1]Department of Genetics, Washington University School of Medicine, St. Louis, MO 63110, USA

[2]Department of Psychiatry, Washington University School of Medicine, St. Louis, MO 63110, USA

Abstract

The gene CUG-BP, Elav-like factor 6 (*CELF6*) appears to be important for proper function of neurocircuitry responsible for behavioral output. We previously discovered polymorphisms in or near *CELF6* may be associated with autism spectrum disorder (ASD) in humans and that the deletion of this gene in mice results in a partial ASD-like phenotype. Here, to begin to understand which circuits might mediate these behavioral disruptions, we sought to establish in what structures, with what abundance, and at which ages Celf6 protein is present in the mouse brain. Using both a knockout-validated antibody to Celf6 and a novel transgenic mouse line, we characterized *Celf6* expression in the mouse brain across development. *Celf6* gene products were present from early in neurodevelopment and into adulthood. The greatest protein expression was observed in distinct nuclei of the diencephalon and neuromodulatory cell populations of the midbrain and hindbrain, with clear expression in dopaminergic, noradrenergic, histaminergic, serotonergic and cholinergic populations, and a variety of presumptive peptidergic cells of the hypothalamus. These results suggest that disruption of *Celf6* expression in hypothalamic nuclei may impact a variety of behaviors downstream of neuropeptide activity, while disruption in neuromodulatory transmitter expressing areas such as the ventral tegmental area, substantia nigra, raphe nuclei and locus coeruleus may have far-reaching influences on overall brain activity.

Keywords

Celf6; neuromodulatory; diencephalon; development; protein expression; immunohistochemistry

Introduction

Mutant mice with deletion of the homologue of the human CUG-BP, Elav-like factor 6 (*Celf6*) gene exhibit a subset of the phenotypes used to assess autism spectrum disorder (ASD)-like behaviors in rodents. Specifically, these mice exhibit early communicative deficits when isolated from the mother and evidence of a resistance to change behavior

Contact: Dr. Joseph D. Dougherty, Washington University School of Medicine, Department of Genetics, Campus Box 8232, 4566 Scott Ave., St. Louis, Mo. 63110-1093, (314) 286-0752, jdougherty@genetics.wustl.edu

Conflict of Interest

None of the authors has any established or potential conflict of interest to declare in relation with the current work.

patterns in an odorant-potentiation hole-poking task (Dougherty et al. 2013). Our group first decided to investigate the link between *Celf6* and ASD symptomology because of an interest in the role of the serotonergic system in the neurobiology and etiology of ASD. We discovered that *Celf6* gene transcripts are enriched in the serotonergic system, that polymorphisms in or near *CELF6* may be associated with autism in humans, and that *Celf6* null mice exhibit a 30% decrease in serotonin (5HT) levels in extracted brain tissue. However, we also saw a trend towards a decrease of norepinephrine (NE) and dopamine (DA) as well; suggesting *Celf6* may have roles outside the serotonergic system and a more widespread analysis of its expression may be warranted.

The *CELF6* gene was first isolated and characterized in 2004 (Ladd et al. 2004), although at that time the gene was called *BRUNOL6* because of the similarity of domain structure of the human Elav family of proteins and the Bruno protein of the *Drosophila melanogaster* (Good et al. 2000). There are two known isoforms of CELF6, which are abundantly expressed in the kidneys and the brain, and expressed at low levels in many other tissues (Ladd et al. 2004). Similar to the five other members of the CELF family, the longest isoform of CELF6 contains three RNA recognition motifs (RRMs) and a divergent domain of unknown function (Ladd et al. 2001; Ladd et al. 2004). In the case of CELF6, the divergent domain contains 268 amino acids and is located between RRM2 and RRM3. The presence of RRMs suggests CELF6 is an RNA-binding protein, and other members of the CELF family have been shown to provide a regulatory role in the alternative splicing of target pre-mRNAs (Barreau et al. 2006), a function that has also been suggested by *in vitro* experiments for this sixth family member (Ladd et al. 2004). CELF-mediated alternative splicing has been shown to influence spermatogenesis, programmed cell death, and inhibitory and excitatory neurotransmission (Ladd 2013; Wagnon et al. 2012). Dysfunction in CELF-mediated alternative splicing has been implicated in myotonic dystrophy type 1 and spinal and bulbar muscular atrophy. Other CELF proteins have also been shown to interact with neurofibromin 1 – the gene that causes neurofibromatosis 1, a syndrome with high comorbidity with autism (Garg et al. 2013), and to interact with the microtubule-associated protein tau and amyloid beta precursor protein, which underlie the neuropathology of Alzheimer's disease (Ladd 2013), as well as additional transcripts that regulate synaptic plasticity and transmission (Wagnon et al. 2012). Along with nuclear RNA splicing, cytoplasmic RNA related functions also have been demonstrated for other CELF family members including the regulation of deadenylation, stability and translation of mature mRNAs (Dasgupta and Ladd 2012).

Previous analysis by RNA dot blot indicated *CELF6* RNA presence in many regions of the adult human brain and in the fetal brain (Ladd et al. 2004), and *in situ* hybridization of *Celf6* RNA indicated expression in the neural tube of the developing chick embryo (Brimacombe and Ladd 2007). However, *Celf6* gene expression has not been characterized in the rodent brain, and protein expression has not been characterized in any species. Before we can begin to understand how the absence of Celf6 is resulting in the ASD-like behavioral phenotypes of the *Celf6* mutant mouse, we need to first establish in what brain structures, with what abundance, and at which ages Celf6 is present in the mouse brain. To achieve this goal, we leveraged both a knockout-validated antibody to Celf6 and a novel transgenic mouse line to characterize *Celf6* expression in the mouse brain across development.

Materials and Methods

Animals

The Washington University Animal Studies Committee approved all experimental protocols. Global *Celf6* knockout (*Celf6*$^{-/-}$) mice were previously generated by deleting exon 4 of the *Celf6* gene (Dougherty et al., 2013). Heterozygous breeding crosses were employed to produce *Celf6*$^{-/-}$ and C57BL/6J wild type (WT) littermates used in experiments below. *Celf6*-YFP BAC (RP24-346B1) transgenic mice were generated as previously described (Doyle et al. 2008) using a single step recombination method (Gong et al. 2010). The generation and breeding of the *Celf6*-YFP transgenic mice used in this study are detailed below (See *Results*).

mRNA extractions and RT-qPCR

Reverse transcriptase quantitative polymerase chain reaction (RT-qPCR) was used to determine temporal transcription of *Celf6* mRNA. Brain tissue from embryonic (E14.5, E17.5), early postnatal (P9) and adult (P60) WT littermates of *Celf6*-YFP mice was used for this experiment (n=3, 3, 3, and 2, respectively). Mice were sacrificed via carbon dioxide asphyxiation and the brains were rapidly removed. One brain hemisphere was homogenized in a glass Teflon homogenizer on ice in RLT buffer containing 10% β-mercaptoethanol and RNA was extracted from tissue with RNeasy Mini Kit columns (Qiagen, Valencia, CA), followed by DNase treatment and RNA purification per the manufacturer's protocol. RNA concentrations were measured with a Nanodrop spectrophotometer and the integrity confirmed by 1% agarose gel electrophoresis. cDNA was synthesized for each sample from 1000 ng of RNA using qScript cDNA SuperMix (Quanta Biosciences, Gaithersburg, MD) per the manufacturer's protocol. qPCR was conducted in an Applied Biosystems ViiA7 instrument (Life Technologies, Grand Island, NY) using the accompanying software with PerfeCTa SYBR Green FastMix (Quanta Biosciences, Gaithersburg, MD). *Celf6* primers were designed to amplify exons 3 and 4 (See Table 1 for sequences). Data were analyzed using the ΔΔCT method and normalized to a *Gapdh* endogenous control. *Mobp* specific primers served as the developmental control as Mobp expression is known to increase across development (Dillman et al. 2013).

Brains from E17.5, P9 and P60 *Celf6*-YFP mice (n=3, 2, and 2, respectively) were processed as above for characterization of transgene mRNA transcription. RT-qPCR was conducted and analyzed as described above with the addition of primers designed to amplify only the endogenous *Celf6* gene (amplifying 320 bp product at the end of exon 11 into exon 12) and YFP primers that amplify only the transgene. All primer sequences used are described in Table 1 and ilustrated in Fig. 4a.

Protein extraction and immunoblotting

Immunoblotting was used to determine temporal expression of Celf6 protein. Embryonic (E17.5), early postnatal (P9) and adult (P60) *Celf6*-YFP transgenic mice were used for this experiment (n=3, 2, and 2, respectively). Four different rabbit anti-Celf6 antibodies (targeted to two different peptides of Celf6) proved unsuitable for western blotting on brain lysates, therefore mouse anti-HA antibody was used to detect the HA tag on the *Celf6*-YFP

transgene to determine the presence of Celf6 protein across different developmental ages. Mouse anti-Gapdh antibody was used to detect Gapdh to confirm equal protein loading across samples.

Mice were sacrificed via carbon dioxide asphyxiation and the brains were rapidly removed. One brain hemisphere was homogenized in a glass Teflon homogenizer on ice in RIPA buffer (2x RIPA incomplete buffer [40 nM TRIS-Cl, Ph 7.0, 0.3 M NaCl, 10 nM EDTA-Na, 2 mM EGTA-Na, 2% NP-40, 2% sodium deoxycholate, 0.2% SDS], 10 nM $NaVO_4$, 0.5 mM NaF, 12.5 IU/mL aprotinin, 0.1% 1 mg/mL leupeptin, proteinase inhibitors [1 Complete EDTA-free mini tablet]). To clarify the samples, each was spun for 20 min at 4°C at 20,817 x g and the pellets discarded. The BCA assay kit (Pierce Protein Biology Products, ThermoScientific, Waltham, MA) and a spectrophotometer were used to determine the concentration of protein in each sample following manufacture's protocol. From each sample, 80 ug of protein was mixed with 5x Sample Buffer (250 mM Tris pH 6.8, 25% β-mercaptoethanol, 50% Glycerol, 0.1% SDS, 0.01% Bromophenol blue in ddH_2O), and heated for 10 min at 90°C. Page gel (Mini-Protean Precast Gels) in buffer (10x TRIS/glycine/SDS buffer diluted in ddH_2O), which was transferred to an activated polyvenadine fluoride membrane equilibrated in buffer (25 mL 10x transfer buffer [39 mM glycine, 48 mM TRIS powder, 0.375% SDS, 20% MeOH, ddH_2O], 175 mL dH_2O, 50 mL MeOH). The blot was incubated in blocking solution (5% non-fat dried milk in TBS with 0.5% Tris [TBST]) for 60 min, then half of the blot was incubated overnight in mouse anti-HA antibody in blocking solution (1:5000 dilution; Pierce Protein Biology Products, ThermoScientific, Waltham, MA), and the other half was incubated for 30 min in mouse anti-Gapdh antibody in blocking solution (1:10,000; Sigma-Aldrich, St. Louis, MO). The next day the blot was washed 3 times for 5 min in TBST, incubated for 120 min in goat anti-mouse HRP secondary antibody in blocking solution (1:5000 dilution; Bio-Rad, Hercules, CA), and washed, again, 3 times for 5 min each in TBST. The Blot then was developed using SuperSignal West Femto Kit (ThermoScientific, Waltham, MA) on HyBlot CL autoradiography film (Denville Scientific Inc, Metuchen, NJ). High resolution (600 DPI) film scans were subjected to densitometry using ImageJ software to determine relative amounts of protein in each lane.

Data analysis for RT-qPCR and immunoblotting

All statistical analyses were performed using the SPSS statistical program for Mac computers, version 21. Factorial ANOVAs were used where appropriate. With a statistically significant interaction between main factors, simple main effects were calculated to provide clarification of statistically significant between-subject differences. Multiple comparisons were Bonferroni adjusted. Tukey's HSD method was used as a post hoc test. Probability value for all analyses was $p < .05$.

Preparation of tissue sections

All brains were processed as previously described (Dougherty et al. 2013). Briefly, mice were killed via carbon dioxide asphyxiation and perfused with approximately 15 mL 0.01 M phosphate buffered saline (PBS) followed by 20 mL of 4% paraformaldehyde in PBS. Immediately following perfusion, the whole brain was removed from each mouse and post-

fixed in perfusate for 24 hr, then cryoprotected in a series of graded sucrose solutions (5–30%) over 48 hr. Each brain was frozen in Neg50 mounting media (Fisher Scientific, Pittsburgh, PA) and serially sectioned (40 μm in thickness) on a cryostat and stored in PBS with 0.1% sodium azide in 4°C until use.

Immunohistochemistry

Immunohistochemical techniques were used to detect regional Celf6 protein expression patterns in the brains of adult mice. Two independent reagents were employed: custom Celf6 polyclonal antibody on WT brain tissue and the *Celf6*-YFP reported mouse line. To determine regional Celf6 expression patterns, brain sections from WT, *Celf6*-YFP, and $Celf6^{-/-}$ adult mice (n=5, 3, 3, respectively) were processed in parallel. Brain tissue from adult $Celf6^{-/-}$ mice was used to confirm antibody specificity. The sections were quenched in methanol containing 3% hydrogen peroxide, then washed 3 times for 5 min each in 0.01 M PBS, followed by a 60 min incubation in blocking solution (5% normal goat serum + 0.2% dry milk in 0.25% triton-X PBS), and then incubated overnight in rabbit anti-Celf6 antibody in blocking solution (1:10,000 dilution; Dougherty et al., 2013) or chicken anti-YFP (anti-GFP antibody that cross reacts with YFP) antibody in blocking solution (1:5000 dilution; Aves Lab Inc, Tigard, OR). The next day the sections were washed 3 times for 5 min in PBS, incubated for 60 min in goat anti-rabbit or anti-chicken biotinylated secondary antibody in blocking solution (1:200 dilution; Jackson Immunoresearch Labs Inc, West Grove, PA), and washed, again, 3 times for 5 min each in PBS. The sections were incubated in the dark with ABC reagents (standard Vectastain ABC Elite Kit, Vector Laboratories, Burlingame, CA) for 60 min, and washed, once again, 3 times for 5 min each in PBS. Finally, the sections were developed in VIP reagents (Vector VIP substrate kit for peroxidase, Vector Labs, Burlingame, CA) for approximately 5 min. The sections were mounted onto 75 × 25 Superfrost Plus slides, dehydrated with a series of graded ethanols and Citrisolv, and cover-slipped with Permount mounting media.

To evaluate developmental Celf6 protein expression, brains from P9 WT and *Celf6*-YFP transgenic pups were processed and immunohistochemical techniques employed as above with both rabbit anti-Celf6 antibody and chicken anti-YFP antibody in blocking solution.

Double-labeling immunofluorescence was used to determine regional cell-type specific Celf6 protein expression as well as a secondary confirmation of endogenous-like expression patterns of the *Celf6*-YFP transgene. Brain sections from WT, *Celf6*-YFP, and $Celf6^{-/-}$ mice were incubated in blocking solution (5% normal donkey serum in 0.25% triton-X PBS) for 30 min then incubated in primary antibody overnight in blocking solution. All primary antibodies are detailed in Table 2. Sections were then washed 3 times for 5 min each in PBS and incubated for 90 min with appropriate Alexa fluorophore-conjugated secondary antibodies and a nuclear dye (DAPI; Invitrogen, Grand Island, NY).

Data analysis for immunohistochemistry

Sections were qualitatively analyzed by using both bright- and darkfield microscopes (Leica DMR; Perkin Elmer UltraView Vox spinning-disk confocal on a Zeiss Axiovert). The relative density and intensity of Celf6 expression in WT, *Celf6*-YFP and $Celf6^{-/-}$ tissues

were determined using Leica DMR microscrope. Brightfield images were captured on a Leica DFC310FX camera mounted to a Leica DM400B microscope using Surveyor software version V7.0.0.6 MT (Objective Imaging, Cambridge, UK) and darkfield images captured on a Perkin Elmer UltraView Vox spinning-disk confocal on a Zeiss Axiovert microscope. Digital raw images were optimized for evenness of illumination and background by using ImageJ (Wayne Rasband, NIH, USA). Anatomical structures were identified according to an adult mouse brain atlas (Franklin and Paxinos). Overall expression was scored by a rubric using both density of cells labeled (+, scattered; ++, light; +++, moderate, or ++++, high) and intensity of signal (+, weak; ++, moderate; or +++, strong). The overall expression score for each region was calculated by multiplying density level by signal intensity. Thus, the expression scores indicate the following: 1 – 2, light expression; 3 – 6, moderate expression; 8 – 9, high expression; and 12, very high expression.

Results

Generation of a Celf6-YFP transgenic mice

Celf6-YFP BAC transgenic mice were generated as previously described (Doyle et al. 2008). Briefly, a BAC (RP24–346B1) covering all known isoforms of the *Celf6* gene, and their putative promoters, was modified to insert a YFP protein with an HA tag in frame with the C-terminus of *Celf6* (Fig. 1a) using a single step recombination method (Gong et al. 2010). While different protein isoforms have alternative N-termini, all known isoforms share this C-terminus (Fig. 1b), and thus all forms would be tagged. BAC modifications were confirmed with southern blotting, and CsCl purified BAC DNA was injected into fertilized FVB mouse eggs. Resultant progeny were screened with PCR for the presence of YFP in the genome to identify founders. Founders were crossed to WT C57BL/6J mice at each generation and transgene expression was evaluated as described below. Two founder lines for *Celf6*-YFP BAC transgenic mice were selected for further analysis (JD2076, JD2078) based on a preliminary anatomical screen for robust expression of the transgene. The preliminarily higher expressing line, JD2076 was subsequently lost due to difficulties in breeding, likely secondary to a morbid obesity. The JD2078 line (heretofore *Celf6*-YFP mice) was used in all experiments. (JD2078 mice showed no overt obesity phenotype, though in-depth behavioral analysis of these mice is a subject of future inquiry). *Celf6*-YFP and WT C57BL/6J breeding crosses were employed to produce *Celf6*-YFP and WT littermates for use in this study. Offspring were genotyped using standard reagents and primers for amplification of the HA-tagged YFP (See Table 1 for sequences).

DNA purification (standard Phenol/Chloroform extraction) and qPCR with copy number standards (1 – 128) were used to estimate the number of transgene copies present in the *Celf6*-YFP tissue samples from different aged animals (E14, E17, P9 and P60). Approximately 10 copies of the transgene were estimated to be present in transgenic animals (Fig. 1c).

Temporal Analysis of Celf6 expression

Celf6$^{-/-}$ mice exhibit early communicative deficits by P8 (Dougherty et al. 2013), indicating the absence of the protein at this developmental age can influence behavior. Therefore, the

mRNA and protein are likely to be present in a normal brain by this age, and thus we centered our analysis on this time point. RT-qPCR and immunoblotting were used to determine embryonic, postnatal and adult presence of *Celf6* gene expression. In order to determine the age-dependent profile of *Celf6* transcription, RT-qPCR was used to examine one full hemisphere of brain tissue from E14.5, E17.5, P9, and P60 WT mice (n=3,3,3 and 2, respectively) for the presence and relative abundance of *Celf6* mRNA.

Celf6 mRNA was detected at all ages assessed with a clear change in mRNA levels with age, $F(3,7) = 8.813$, $p = .009$ (Fig. 2a). The observed predominant age for *Celf6* mRNA levels was E17.5, with a 1.8-fold increase from E14.5 ($p = .042$). A marginally significant 1.7-fold decrease in Celf6 mRNA was observed by P9 ($p = .058$) and a 3.5-fold decrease by P60 ($p = .007$). As expected, our positive developmental control, the myelinating oligodendrocyte marker *Mobp* mRNA levels changed with age, $F(3,7) = 115.794$, $p = .000003$ (Fig. 2b), with *Mobp* mRNA present only at postnatal ages. These results indicate *Celf6* mRNA to be most abundant during development, specifically at late-prenatal ages.

To determine changes in Celf6 protein levels across neural development, an immunoblot was conducted on one full hemisphere of brain tissue from E17.5, P9 and P60 *Celf6*-YFP mice. Four different rabbit anti-Celf6 antibodies (targeted to two different peptides of Celf6) proved unsuitable for western blotting on brain lysates, therefore mouse anti-HA antibody was used to detect the HA tag on the *Celf6*-YFP transgene. Tissue from a P60 WT brain was used as a control for specificity of the antibody. The western blot indicated Celf6 protein was present by later embryonic ages and more abundant during developmental time points than adulthood (Fig. 3a). The long and short Celf6 isoforms (75 and 63 kDa, respectively, when fused with YFP-HA) were both present on the immunoblot at all ages, and absent from WT lysate. The HA antibody also produced a protein band at 50 kDa, which is non-specific binding as it was also present in the WT lysate. Densitometric analysis of *Celf6*-YFP bands (normalized to within-sample Gapdh) across ages statistically confirmed Celf6 protein levels at both E17.5 and P9 were greater than that at P60, $F(2,4) = 30.495$, $p = .004$ (Fig. 3b). The relative intensity of the long isoform was greater than that of the short isoform at all ages. Specifically, the pixel density of the long isoform was 1.7, 1.9, and 1.7 times that of the short isoform for P17, P9, and P60, respectively (data not shown).

As the transgenic Celf6-YFP protein was used as a proxy for the expression the endogenous protein, we next sought to confirm that the age-dependent difference in protein levels was driven by age-dependent differences in transcription, and that transgene expression mirrors endogenous *Celf6* expression. Thus, RT-qPCR was used to assess mRNA levels in WT and *Celf6*-YFP transgenic mice across several ages. Primers were used as above that amplified *Celf6* mRNA regardless of genetic origin (total *Celf6* mRNA) as well as those that amplified only the endogenous *Celf6* gene mRNA (amplifying the very end of exon 11 and beginning of exon 12, which are not included in the transgene mRNA because of a strong PolyA signal) and YFP primers that amplified only the transgenic *Celf6* mRNA (Table 1; Fig. 4a).

A similar pattern emerges for all *Celf6* gene products (Fig. 4b–d). Consistently and regardless of genetic origin, *Celf6* mRNA levels are higher at age E17.5 and P9 than P60 (Fig. 4b–d). For mRNA amplified by primers that recognized both the endogenous copy and

the transgenic copy (total), a significant age x genotype interaction, $F(2,7) = 12.953$, $p = .004$, revealed that within the WT brains, $F(2,7) = 21.826$, $p = .011$, and transgenic brains, $F(2,7) = 90.203$, $p = .0001$, more total *Celf6* mRNA was present in E17.5 and P9 compared to P60, $p < .045$ (Fig. 4b). Unlike in the WT mice brains, however, the difference between E17.5 and P9 total *Celf6* mRNA held up to Bonferroni correction in the transgenic mice brains, $p = .0008$.

As expected, the addition of the extra copies in the transgene resulted in greater *Celf6* mRNA levels total than that produced by the endogenous *Celf6* gene alone. Between-genotype analysis revealed more total *Celf6* mRNA in the E17.5 and P9 transgenic brains than the age-matched WT brains, $F(1,7) = 88.556$, $p = .0004$ and $F(1,7) = 18.655$, $p = .037$, respectively (Fig. 4a). The means also suggested more total *Celf6* mRNA in the P60 transgenic brain than the P60 WT brain; however, the result was not significant after Bonferroni correction. Furthermore, the main analysis also yielded a significant main effect of genotype, $F(1,7) = 90.856$, $p = .00003$, indicating that, when collapsed across ages, the transgenic brains contained more total *Celf6* mRNA compared to the WT brains. These data imply that while more *Celf6* mRNA was present in the transgenic mouse brain due to transcription from the endogenous copy and the transgene copies, the age-dependent pattern of total *Celf6* mRNA was similar between the WT and *Celf6*-YFP transgenic mice.

As many RNA binding proteins are known to regulate their own mRNAs, we next focused on the primers designed to amplify only the endogenous gene, to understand if the presence of the transgene might influence the levels of endogenous *Celf6* mRNA. The age-dependent patterns observed for transgene + endogenous (total) *Celf6* mRNA in the *Celf6*-YFP mice were mirrored by the patterns for endogenous mRNA only and transgene mRNA only. Analysis of the *Celf6*-YFP samples revealed significant main effects of age for both endogenous, $F(2,3) = 842.686$, $p = .00008$ (Fig. 4c), and transgenic, $F(2,3) = 35.788$, $p = .008$ (Fig. 4d), mRNA levels. Regardless of genetic origin, more mRNA was observed in E17.5 tissue compared to both P9 and P60, $p < .008$, and in P9 compared to P60, $p < .036$. However, transgenic mRNA differences reached marginal significance between E17.5 and P9, $p = .070$. The similarity of age-dependent Celf6 mRNA levels between primer sets, and particularly between genotypes, suggested levels of the Celf6 transgene mRNA across ages were similar to those of the endogenous Celf6 gene mRNA. Furthermore, these data indicated the transgene did not influence the age-specific pattern observed with endogenous *Celf6*. We can therefore concludethe age-dependent difference in protein levels quantified through detection of the transgenic protein are likely to accurately reflected the age-dependent difference in endogenous Celf6 protein levels.

Spatial analysis of Celf6 Expression

To understand the circuits most likely to mediate the behavioral disruptions seen in the *Celf6*$^{-/-}$ mice, we next sought to characterize the spatial expression of Celf6 protein throughout the brain using two independent reagents: the custom Celf6 polyclonal antibodies and the transgenic *Celf6*-YFP reporter mouse line. WT tissue was processed using custom Celf6 polyclonal antibodies with *Celf6*$^{-/-}$ tissue providing confirmation of antibody specificity. *Celf6*-YFP tissue was processed with commercially available anti-YFP

antibody (Aves Lab Inc, Tigard, OR) allowing for independent study of *Celf6* promoter activity. Immunohistochemical staining for Celf6 protein (both endogenous and transgenic) was examined by light microscopy to determine the protein's regional distribution. The cellular colocalization of Celf6 protein with various neuromodulatory neurotransmitters was determined by double-labeling immunofluorescence and confocal microscopy.

Celf6 is widely expressed throughout the adult mouse brain. Celf6 protein levels vary widely in the density of cells labeled and the intensity of the signal throughout various regions of the mouse brain (Table 3). Across five WT replicates and three *Celf6*-YFP transgenic replicates, the broad overall pattern shows presence of Celf6 protein throughout the brain at low intensity of expression. However, within distinct regions of the brain, Celf6 protein is expressed much more robustly (Figs. 5a–l & 6a–l). Various nuclei of the diencephalon and neuromodulatory cell populations of the midbrain and hindbrain contained the highest expression levels while more moderate expression was observed in areas of the forebrain with scattered areas of more intense signal in the cortex. The cerebellum was the only area largely devoid of expression. No equivalent pattern was seen in the knockout mouse brain sections examined with the same antibody in parallel (n=3, Fig. 7a–l). Throughout the brain, The majority of cells positive for Celf6 protein exhibit very weak signal intensity, while a limited number of areas, discussed below, exhibited stronger signal intensity. All regions showing any signal are listed, along with summary expression values, in Table 3. We next carefully examined in detail each region with detectable Celf6 expression.

Forebrain—Some Celf6 protein signal was detectable in almost every major region of the forebrain with varying degrees of intensity and density of expression. Overall, Celf6 protein was expressed at relatively low levels in many areas, including the cortex, however, distinct regions, particularly in the diencephalon, showed higher relative expression, suggesting these areas require more Celf6 activity for proper function.

Within the neocortex, Celf6 protein was detected with varying densities within all laminar layers and across all regions of the cortex. Sparse Celf6-positive cells were observed in layer 1, yet with moderate density and low intensity, and Celf6-positive cells were observed throughout cortical layers 2/3, 4, 5, and 6a/b. More intense signal was observed in various neocortical regions, highlighted as follows: Medially in the anterior cortex, Celf6 was moderately expressed. Protein was observed in the prelimbic, medial orbital, and infralimbic cortices. Scattered cells of high intensity Celf6 protein signal were observed in both the dorsal and ventral tenia tecta but only in layers 2 and 3. The anterior olfactory area showed scattered, intense signal of Celf6 protein. Laterally in the more anterior portions of the cortex, including the dorsal surface, low expression of Celf6 was observed. Celf6 protein was present throughout areas 1 and 2 of the cingulate cortex, both the primary and secondary motor and somatosensory cortices, as well as the gustatory cortex, which includes the granular, dysgranular, and (dorsal, ventral and posterior) agranular insular cortices. Celf6 protein was observed at moderate expression levels in the pyramidal layer of the piriform cortex of the olfactory system, but in only scattered cells of the polymorph layer and was absent in the molecular layer. In posterior regions of the cortex, low expression of Celf6 was observed (Figs. 5a, 6a). These areas include the primary and secondary visual (V1, V2) and auditory cortices (Au1, AuD, AuV), and temporal (TeA) and parietal association areas.

Similar expression patterns as reported above were observed in the hippocampal cortex, except for the granular and pyramidal cell layers of the hippocampus proper (Figs. 5a, 6a). Low expression of Celf6 was observed in the parahippocampal regions of the perirhinal, ectorhinal, and entorhinal cortices. Cells with moderately intense signal were scattered within these areas. Celf6 protein was located throughout the cells within the granular cell layer of the dentate gyrus and with light density in the polymorph layer, but was absent from the molecular layer. Within the hippocampus proper, light expression was observed in cells of the oriens, radiatum (Rad), and lacunosum molecular (LMol) layers across Fields CA1–3 and in the subiculum. Expression was slightly higher in the ventral hippocampus relative to the dorsal hippocampus. Light Celf6 expression overall was observed in the amygdalar regions. The medial amygdaloid nucleus showed the greatest expression, with moderate density but relatively weak intensity. Scattered cells of the basolateral and lateral amygdaloid nuclei showed more intense protein signal. These expression patterns suggested greater Celf6 activity within areas of the hippocampus compared to amygdalar nuclei or cortex.

Celf6 expression was more dense and intense in the subpallial structures relative to cortical areas. The highest expression was observed in the regions comprising the basal forebrain, including the bed nuclei of the stria terminalis, diagonal band nucleus, lateral and medial septal nuclei (MS), substantia innominata (SI) and the nuclei of the horizontal (HDB) and vertical limbs of the diagonal band (VDB; Figs. 5b,f & 6b,f). Double-labeling immunofluorescence revealed colocalization of Celf6 protein with choline acetyltransferase (ChAT), an enzyme responsible for the synthesis of the neurotransmitter acetylcholine. This indicates Celf6 is expressed in the cholinergic neurons of the basal forebrain (Fig. 8a, b) that innervate the cortex, hippocampus, and other limbic structures. Areas within the striatum contained scattered cells with moderate Celf6 protein signal. These areas included the caudoputamen (CP), lateral accumbens shell (LAcbSh), and nucleus accumbens shell (AcbSh; Figs. 5b–c, 6b–c). Within the CP (Fig. 8c), the moderate expression of Celf6 protein was found in the cholinergic interneurons neurons; however, Celf6 protein was observed in very few cholinergic neurons of the Acb (Fig. 8d). Similar expression of Celf6 protein was observed in another area of the basal ganglia, the external and internal segments of the globus pallidus (GP), where Celf6 was observed in both the sparse cholinergic projection neurons and the more common non-cholinergic cells (Fig. 8e).

Within the diencephalon, distinct nuclei showed the highest expression of Celf6 protein found in the brain outside of the locus coeruleus (LC). High expression was also observed in many nuclei, mainly those of the hypothalamus, in addition to a very high expression in the epithalamus. Moderate Celf6 protein expression was observed in the prethalamus zona incerta, which overlapped highly with the A13 population of dopaminergic cells of this area (Fig. 9a). Within the thalamus, Celf6 was expressed densely, although with lower intensity of signal, in the central medial nucleus, medial geniculate complex, paraventricular nucleus (PV; Figs. 5d, 6d), peripeduncular nucleus, and the parvicellular part of the subparafascicular nucleus of the thalamus. Sitting atop the dorsal surface of the thalamus is the epithalamus, which is composed of the habenulae. Very high expression was observed in the dorsal aspect of the lateral habenula (LHb) and the lateral and dorsal aspects of the medial habenula (MHb; Figs. 5d, 6d). Celf6 protein was located outside of the densely-

packed population of cholinergic neurons of the MHb (Fig. 9d). Interestingly, all areas connected to the LHb and MHb by afferent and efferent pathways (Puelles et al. 2012) also expressed Celf6 protein, and most at relatively high levels, including the basal forebrain, hypothalamus, ventral tegmental area (VTA), substantia nigra, and raphe nuclei.

In all, twenty-eight nuclei and areas of the hypothalamus contained Celf6 expression, with almost all at moderate to high levels. All hypothalamic areas of expression are listed in Table 3. The nuclei with the highest expression are in close proximity to the ventral portion of the third ventricle. Specifically, these include the paraventricular (Pa) and periventricular nuclei (Pe), the arcuate hypothalamic (Arc) and supraoptic nuclei (SO; Figs. 5e, g & 6e, g), which also contain the small dopamingeric cell populations A12 and A14 (Fig. 9b, c). The ventrolateral preoptic nucleus (VLPO) and the medial tuberal nucleus (MTu) both contained intense Celf6 signal, but in less dense population of cells (Figs. 5f, g & 6f, g). Celf6 presence was also confirmed in neuromodulatory peptide populations of the hypothalamus by double-labeling immunofluorescence. Previously, our group demonstrated Celf6 protein was present in all the orexinergic cells of the lateral hypothalamic area (LH) (Dalal et al. 2013). Celf6 also labeled the histaminergic (histidine decarboxylase [HDC]-positive) cells of the MTu and LH (Fig. 9e, f). Overall, the high levels of Celf6 protein expression in the diencephalic areas, especially the hypothalamus, suggested Celf6 activity might be important to the proper control of homeostasis and motivated behaviors that are attributed to these regions.

Midbrain and Hindbrain—The midbrain and the hindbrain house most of the monoaminergic neuromodulatory cell populations that innervate the forebrain. Within these areas, it is the neuromodulatory cell populations that most highly expressed Celf6 protein. Indeed, outside of the hypothalamus and epithalamus, the highest expression of Celf6 was found within the noradrenergic and serotonergic nuclei of the hindbrain.

The highest overall expression in the midbrain and hindbrain areas was observed in the LC (Figs. 5h, 6h). This dense population of cell bodies is the largest noradrenergic cell population (A6) in the mouse brain and produces ~90% of the noradrenergic projections (Watson 2012a). Confocal microscopy confirmed Celf6 protein was colocalized in the neurons of this cell population with tyrosine hydroxylase (Th; Fig. 10a), the rate-limiting enzyme in the synthesis of DA and NE. Celf6 protein also was present with moderate overall expression in the NE-synthesizing cells (A5) of the superior olivary complex (data not shown), the noradrenergic cells (A7) of the caudal part of the pontine reticular nucleus (PnC; Fig. 10b), in the few NE-synthesizing cells (A2) found in the dorsal motor nucleus of the vagus nerve (10N; Fig. 10c), and in the NE-synthesizing cells (A1) of the lateral reticular nucleus (LRt; data not shown). Celf6 also was observed in non-Th-synthesizing cells of these regions. Taken together, these expression patterns revealed that Celf6 is expressed in, but not isolated to, most noradrenergic cell populations of the hindbrain.

Consistent with our initial screen for mRNAs highly translated in serotonergic neurons (Dougherty et al. 2013), Celf6 protein also was expressed in all the serotonergic raphe nuclei. Celf6 expression in the raphe nuclei as a whole was moderate to high. High expression was observed in the caudal raphe group (B1-B4; Figs. 5l, 6l), the raphe pallidus

(RPa), obscurus (RO), and magnus (RMg). In the rostral group of raphe nuclei (B6-B9), high Celf6 expression was observed in the dorsal raphe (DR; Figs. 5j, 6j) and the median and caudal linear raphe nuclei (MnR; Figs. 5k, 6k). Celf6 antibody colocalization with an antibody raised against tyrosine hydroxylase 2 (Tph2), an enzyme specific to 5HT synthesis in the CNS, was confirmed with confocal microscopy verifying Celf6 protein expression in the serotonergic neurons of these populations (Fig. 10d–g). The Celf6-positive cells of the raphe were not limited to those also synthesizing 5HT. For example, in the DR, while most Celf6-positive cells were the 5HT neurons, additional Celf6 cells were also present. There were also adjacent cells expressing Celf6 that were more likely part of the periaqueductal gray (PAG) or the acetylcholine-producing cells of the laterodorsal tegmental nucleus (LDTg; Figs. 5j, 6j; see below).

Unlike cell populations synthesizing NE and 5HT, DA-synthesizing cells are not limited to the posterior aspect of the brain. DA-synthesizing cells can be found in distinct nuclei of the hypothalamus, as discussed above. However, the largest cell groups, which give rise to two of the three major dopaminergic projections, are found in the midbrain. Recent gene expression studies suggest these cell populations actually derive from hindbrain tissue during development (Watson 2012a). There are three populations of dopaminergic cells in the mindbrain: the substantia nigra pars compacta (SNc; A9), VTA (A10) and the retrorubral field (A8) of the midbrain reticular nucleus. Immunohistochemistry revealed moderate expression of Celf6 protein in all three regions (Figs. 5i, 6i). Specifically, Celf6 was present in all dopaminergic cells, but less abundantly, displayed as lower intensity, compared to the noradrenergic and serotonergic cells discussed above. Double-labeling immunofluorescence confirmed Celf6 protein was present in the Th-expressing, and, therefore, DA-synthesizing, neurons of these regions. Confocal microscopy revealed Celf6 appeared in the majority of the Th-expressing cells of SNc and VTA (Fig. 10h–i). The level of protein colocalization was similar to that observed in the raphe nuclei.

The regions of the midbrain and hindbrain that contain high expression of Celf6 protein outside of the monoaminergic populations are the Edinger-Westphal nucleus (EW; Figs. 5i, 6i), the nucleus ambiguus (Amb) and the taste relay station of the parabrachial nucleus, lateral division. Immunofluorescence double-labeling revealed the Celf6-expressing neurons of the EW overlapped with only a few of the cholinergic preganglionic cells, which may actually have been a few of the motor neurons of the oculomotor nucleus (3N) that lies just lateral to the EW (Fig. 11a). The Celf6 cells were more likely the EW neurons containing neuropeptides that are associated with stress-responses or feeding such as urocortin (May et al. 2008; Watson 2012b). However, the Celf6-expressing neurons of the Amb were the cholinergic motor neurons (Fig. 11b) and as were those of the parabigeminal nucleus (data not shown). Unlike the serotonergic and dopaminergic cell groups, Celf6 was not observed in all cholinergic mindbrain and hindbrain populations. Celf6 was present with light to moderate expression in the centrally projecting neuromodulatory cholinergic cells of the pedunculopontine (pedunculotegmental) nucleus (PTg; Fig. 11c), the LDTg (Fig. 11d), the interpolar part of the spinal nucleus of the trigeminal (data not shown) and in some scattered cholinergic cells of the magnocellular part of the medial vestibular nucleus (MVeMC; Fig. 11e). Protein was not observed in other cholinergic cell groups such as the dorsal tegmental nucleus (data not shown), and posterodorsal tegmental nucleus (PDTg; Fig. 11f), or other

prominent motor nuclei such as the facial motor nucleus and motor trigeminal nucleus. Overall, our results indicate that Celf6 was not present in just one type of cholinergic hindbrain population, but resides in a subset of neuromodulatory, motor, and sensory cholinergic neurons.

Taken together, the findings in the neuromodulatory cell populations of the midbrain and hindbrain showed that Celf6 protein was the most abundant in the noradrenergic, serotonergic and dopaminergic cells overall. Celf6 expression was observed in more acetylcholine-expressing cells of the forebrain compared to the hindbrain, yet expression was not as intense in any cholinergic cell type compared to the monoaminergic neuromodulatory populations. Other areas of the midbrain and hindbrain regions contained Celf6 protein outside of those that synthesize neuromodulatory neurotransmitters. For a complete list of midbrain and hindbrain regions containing Celf6 protein expression, see Table 3.

Finally, both *Celf6* mRNA and protein are more abundant in the developmental brain (P9) compared to the adult brain. To determine if this greater abundance of protein was expressed in areas outside of those seen in the adult brain, immunohistochemical techniques were employed as above. Anti-Celf6 antibody staining in WT and *Celf6*-YFP tissue and anti-YFP antibody staining in *Celf6*-YFP tissue confirmed Celf6-positive cell patterns in the P9 brain exactly matched that of the adult brain (data not shown). These findings, along with the age-dependent levels of Celf6 protein indicate that Celf6 was present in the same areas of the brain from development through adulthood and that only the relative abundance of the protein, likely dependent on the amount of mRNA transcribed, changed with age.

Subcellular localization of Celf6

We examined the subcellular localization of Celf6 protein to get an idea of what function this RNA-binding protein may have in the cell. Some *in vitro* evidence suggests Celf6 may have splicing activity, similar to other CELF proteins (Barreau et al. 2006; Ladd et al. 2004), in which case it would be primarily localized to the nucleus, where splicing occurs. High magnification confocal microscopy was used to determine subcellular localization of Celf6 protein. Cells were stained with anti-Celf6 antibodies and the nuclear marker DAPI. As seen in Fig. 12a, Celf6 protein was present in both the nucleus and the cytoplasm of the cell. Complete colocalization was observed between anti-Celf6 antibody and anti-NeuN antibody (Fig. 12b). NeuN (Rbfox3), one of the Fox family of splicing factors (Underwood et al. 2005), has multiple isoforms localized to both the nucleus and cytoplasm of neurons in specifically post-mitotic neurons and has known splicing actions (Dredge and Jensen 2011; Lind et al. 2005). The subcellular localization of Celf6 protein was not inconsistent with a role in alternative splicing, however further studies are needed to determine if splicing is indeed a function of Celf6 in the brain, and there was clearly abundant Celf6 outside of the nucleus where splicing occurs. CELF1 and CELF2 have been demonstrated to carry out functions in the cytoplasm of the cell that regulate adenylation, transcript stability, and translation (Dasgupta and Ladd 2012). The observation of Celf6 in the cytoplasm in this study suggests that this family member might also be involved in the regulation of important cytoplasmic functions. Celf6 labeling also was observed in neurites (Fig. 12a). This finding,

along with the RRMs indicating that Celf6 is a RNA-binding protein, suggested Celf6 also might be involved in the transportation of mRNA to other areas of the cell.

Discussion

We have conducted a thorough analysis of the temporal and spatial expression of *Celf6* in the mouse brain using two complementary approaches. Antibodies on WT and transgenic brains revealed similar regional patterns of Celf6 protein expression and the same age-dependent pattern of *Celf6* mRNA levels. Both *Celf6* mRNA and Celf6 protein levels, in transgenic and WT mice, were higher at developmental ages compared to adulthood. The data suggests, however, that *Celf6* transcriptional activity may be greatest during late embryonic ages while the protein levels likely peak during the first two weeks postnatal. These findings also reveal that despite an increase in gene copy number and total *Celf6* mRNA levels over WT in the *Celf6*-YFP transgenic mouse brain, the transgenic Celf6 protein spatially and temporally resembles that of the endogenous *Celf6* protein. Thus, the novel transgenic line generated here may also be of use in future biochemical studies of Celf6 protein and RNA interacting partners in the brain.

Prior studies demonstrated relatively high expression of *Celf6* RNA in the human brain (Ladd et al. 2004), and the presence of *Celf6* RNA early in development in the chick brain (Brimacombe and Ladd 2007), but no work had been done previously in rodent or with cellular resolution of the protein in any species. The study here confirmed that *Celf6* gene expression occurrs during neurodevelopment, as early as E14, and demonstrated Celf6 protein is located in many regions of the adult mouse brain. Consistent with our prior microarray results (Dalal et al. 2013; Dougherty et al. 2013), the highest expression of Celf6 was observed in the regions synthesizing neuromodulatory neurotransmitters such as acetylcholine, DA, 5HT, and NE. These areas include the basal forebrain, VTA, SNc, raphe nuclei and LC. Disruption of these cell populations can potentially impact many behaviors as they project widely and their activity influences that of the entire brain. High expression was also observed in medial hypothalamic nuclei adjacent to the third ventricle, the area of the brain responsible for maintaining motivated behaviors. Albeit often weak and sparse, Celf6 was also observed in every major brain region, although the cerebellum was particularly devoid of expression.

It is a reasonable assumption that the circuits mediating the behaviors disrupted in the *Celf6*$^{-/-}$ mice (Dougherty et al. 2013) may have some conserved counterparts in humans. The neurocircuitry disrupted in ASD remains an important unknown of this disorder, however, there are brain regions and cell types implicated in the different symptom domains (Maloney et al. 2013). Communication deficits are tightly coupled with the social disruptions at the core of ASD, but distinct regions are thought to play a role in communication. In mice, areas including Amb, solitary nucleus, PAG, motor cortices, and striatum have been suggested to be involved in ultrasonic vocalization behaviors (Arriaga et al. 2012). Of these areas, Amb, a motor nucleus, showed high expression of Celf6 protein, yet the decrease in overall vocalization amount seen in the Celf6 mutants did not in any way alter the temporal or spectral features of the remaining calls. This is in contrast to mutations specifically disrupting a brainstem motor circuit (Tupal et al. 2014), which resulted in

perturbed temporal structure of call phrasing, but a normal overall amount of calls. This argues against the *Celf6*$^{-/-}$ phenotype being primarily a result of motoric deficits, and suggests there may be some upstream motivational deficit, despite a loss of the protein in the Amb. Disruption in the function of the dorsal striatum, a structure associated with behavioral motivation across species, has been suggested to underlie the repetitive interests and resistance to change behavior patterns observed in ASD patients (Maloney et al. 2013; Sears et al. 1999). Celf6 protein was not highly expressed in the output neurons of this region (the medium spiny neurons that make of the large proportion of the cells here); however, there was robust expression in both the striatal cholinergic interneurons and the dopaminergic inputs to this structure.

The high expression in nuclei of the hypothalamus, a key brain region in the regulating a variety of fundamental behaviors and organismal physiology, suggests Celf6 protein also may be important to the proper control of aspects these phenotypes, such as feeding, or regulation of the endocrine system. Indeed, a high expressing transgenic line did exhibit a morbid obesity, although the line was lost before it could be thoroughly evaluated. The hypothalamus also is notable for the amount of peptide neurotransmitters found there and Celf6 expression is found in many nuclei also containing neuropeptide expression. This suggests this RNA-binding protein could have some important connection to neuropeptide activity.

It is possible that the absence of Celf6 in the raphe, VTA or LC is also impacting behavioral performance of the mice due to the far-reaching influence these cell populations have on overall brain function (Maloney et al. 2013). The serotonergic system, for example, has been implicated in the etiology of a subset of ASD cases. Decreasing 5HT in human ASD patients through tryptophan depletion can exacerbate repetitive thoughts and behaviors (Cook and Leventhal 1996; McDougle et al. 1993). Mice lacking Tph2, and therefore brain 5HT brain, exhibit repetitive behaviors (Alenina et al. 2009; Angoa-Perez et al. 2012; Kane et al. 2012; Mosienko et al. 2012). Thus, deleting Celf6 protein from the raphe nuclei may reveal a role of Celf6 in this structure for resistance to change behaviors of the knockout.

Members of the CELF family of proteins have been shown to provide a regulatory role in the alternative splicing of target pre-mRNAs (Barreau et al. 2006), which influences many cellular functions and the dysfunction of which has been implicated in the pathology of various diseases (Garg et al. 2013; Ladd 2013; Wagnon et al. 2012). Along with nuclear RNA splicing, members of the CELF family of proteins have been shown have cytoplasmic RNA related functions including the regulation of deadenylation, stability and translation of mature mRNAs (Dasgupta and Ladd 2012). However, these cytoplasmic functions have only been demonstrated for CELF1 and CELF2, and to some extent CELF4 (Wagnon et al. 2012). It is unclear whether the other three family members also provide these functions. Our subcellular localization experiments demonstrated Celf6 is present in the nucleus and the cytoplasm of cells of the brain. The nuclear localization is consistent with previous *in vitro* findings indicating Celf6 has slicing activity (Ladd et al. 2004). However, the extensive signal outside the nucleus indicates that Celf6 may also regulate RNA in the cytoplasm. Further biochemical studies will be required to examine these putative functions for Celf6.

In general, future studies with conditional deletion using the Cre-Lox recombination strategy will enable us to determine which of these regions that normally express Celf6 protein may mediate which of the ASD-like behaviors of the knockout model. *Celf6* gene expression is present during neurodevelopment and through to adulthood, thus employing an inducible Cre-Lox strategy to delete Celf6 gene activity after neurodevelopment will allow us also to address whether the behaviors observed in the *Celf6*$^{-/-}$ mouse are a result of the absence of the Celf6 protein at any age, or due to changes during neurodevelopment that resulted from the absence of the protein. Overall, the protein is found widely in the brain, yet with distinct regions of markedly higher expression, suggesting this RNA-binding protein may influence behavior through these specific brain circuits.

Acknowledgements

The authors would like to thank Arthur Loewy, Paul Gray, Nathaniel Heintz, and Cristina de Guzman Strong for equipment, reagents and discussion. We would also like to thank Heifen Feng, Juliet Zhang, and Afua Akuffo for technical assistance. Funding was provided by R21MH099798, DA038458-01, R00NS067239 to JDD, and an ACE network grant R01MH100027.

Glossary

10N	dorsal motor nucleus of vagus
3N	oculomotor nucleus
A12	A12 dopamine cells
A13	A13 dopamine cells
A14	A14 dopamine cells
Acb	accumbens nucleus
AcbC	accumbens nucleus, core
AcbSh	accumbens nucleus, shell
AHA	anterior hypothalamic area, anterior part
Amb	ambiguus nucleus
Arc	arcuate hypothalamic nucleus
Au1	primary auditory cortex
AuD	secondary auditory cortex, dorsal area
AuV	secondary auditory cortex, ventral area
CP	caudoputamen (striatum)
DM	dorsomedial hypothalamic nucleus
DR	dorsal raphe nucleus
EW	Edinger-Westphal nucleus
GP	globus pallidus

HDB	nucleus of the horizontal limb of the diagonal band
IO	inferior olivary nucleus
LC	locus coeruleus
LDTg	laterodorsal tegmental nucleus
LH	lateral hypothalamic area
LHb	lateral habenular nucleus
LMol	lacunosum moleculare layer of the hippocampus
LPO	lateral preoptic area
LRt	lateral reticular nucleus
MHb	medial habenular nucleus
MnR	median raphe nucleus
MPA	medial preoptic area
MS	medial septal nucleus
MTu	medial tuberal nucleus
MVeMC	medial vestibular nucleus, magnocellular part
Pa	paraventricular hypothalamic nucleus
PAG	periaqueductal gray
PDTg	posterodorsal tegmental nucleus
Pe	periventricular hypothalamic nucleus
PnC	pontine reticular nucleus, caudal part
PTg	pedunculotegmental nucleus
PV	paraventricular thalamic nucleus
Rad	radiatum layer of the hippocampus
RMg	raphe magnus nucleus
RO	raphe obscurus nucleus
RPa	raphe pallidus nucleus
SI	substantia innominata
SIB	substantia innominata, basal part
SNc	substantia nigra, compact part
SO	supraoptic nucleus
TeA	temporal association cortex
V1B	primary visual cortex, binocular area

VDB	nucleus of the vertical limb of the diagonal band
VLPO	ventrolateral preoptic nucleus
VTA	ventral tegmental area

References

Alenina N, et al. Growth retardation and altered autonomic control in mice lacking brain serotonin. Proceedings of the National Academy of Sciences of the United States of America. 2009; 106:10332–10337. [PubMed: 19520831]

Angoa-Perez M, et al. Genetic depletion of brain 5HT reveals a common molecular pathway mediating compulsivity and impulsivity. Journal of neurochemistry. 2012; 121:974–984. [PubMed: 22443164]

Arriaga G, Zhou EP, Jarvis ED. Of mice, birds, and men: the mouse ultrasonic song system has some features similar to humans and song-learning birds. PloS one. 2012; 7:e46610. [PubMed: 23071596]

Barreau C, Paillard L, Mereau A, Osborne HB. Mammalian CELF/Bruno-like RNA-binding proteins: molecular characteristics and biological functions. Biochimie. 2006; 88:515–525. [PubMed: 16480813]

Brimacombe KR, Ladd AN. Cloning and embryonic expression patterns of the chicken CELF family Developmental dynamics : an official publication of the American Association of Anatomists. 2007; 236:2216–2224. [PubMed: 17584860]

Cook EH Jr, Leventhal BL. The serotonin system in autism. Curr Opin Pediatr. 1996; 8:348–354. [PubMed: 9053096]

Dalal J, et al. Translational profiling of hypocretin neurons identifies candidate molecules for sleep regulation Genes & development. 2013; 27:565–578. [PubMed: 23431030]

Dasgupta T, Ladd AN. The importance of CELF control: molecular and biological roles of the CUG-BP, Elav-like family of RNA-binding proteins. Wiley interdisciplinary reviews RNA. 2012; 3:104–121. [PubMed: 22180311]

Dillman AA, et al. mRNA expression, splicing and editing in the embryonic and adult mouse cerebral cortex. Nat Neurosci. 2013; 16:499–506. doi:http://www.nature.com/neuro/journal/v16/n4/abs/nn.3332.html#supplementary-information. [PubMed: 23416452]

Dougherty JD, et al. The disruption of Celf6, a gene identified by translational profiling of serotonergic neurons, results in autism-related behaviors. J Neurosci. 2013; 33:2732–2753. [PubMed: 23407934]

Doyle JP, et al. Application of a translational profiling approach for the comparative analysis of CNS cell types. Cell. 2008; 135:749–762. [PubMed: 19013282]

Dredge BK, Jensen KB. NeuN/Rbfox3 nuclear and cytoplasmic isoforms differentially regulate alternative splicing and nonsense-mediated decay of Rbfox2. PloS one. 2011; 6:e21585. [PubMed: 21747913]

Franklin, KBJ.; Paxinos, G. Paxinos and Franklin's The mouse brain in stereotaxic coordinates. Fourth edition.

Garg S, Green J, Leadbitter K, Emsley R, Lehtonen A, Evans DG, Huson SM. Neurofibromatosis Type 1 and Autism Spectrum Disorder. Pediatrics. 2013; 132:e1642–e1648. [PubMed: 24190681]

Gong S, Kus L, Heintz N. Rapid bacterial artificial chromosome modification for large-scale mouse transgenesis. Nat Protocols. 2010; 5:1678–1696. [PubMed: 20885380]

Good PJ, Chen Q, Warner SJ, Herring DC. A family of human RNA-binding proteins related to the Drosophila Bruno translational regulator. The Journal of biological chemistry. 2000; 275:28583–28592. [PubMed: 10893231]

Kane MJ, Angoa-Perez M, Briggs DI, Sykes CE, Francescutti DM, Rosenberg DR, Kuhn DM. Mice genetically depleted of brain serotonin display social impairments, communication deficits and repetitive behaviors: possible relevance to autism. PloS one. 2012; 7:e48975. [PubMed: 23139830]

Ladd AN. CUG-BP, Elav-like family (CELF)-mediated alternative splicing regulation in the brain during health and disease. Molecular and cellular neurosciences. 2013; 56:456–464. [PubMed: 23247071]

Ladd AN, Charlet N, Cooper TA. The CELF family of RNA binding proteins is implicated in cell-specific and developmentally regulated alternative splicing. Molecular and cellular biology. 2001; 21:1285–1296. [PubMed: 11158314]

Ladd AN, Nguyen NH, Malhotra K, Cooper TA. CELF6, a member of the CELF family of RNA-binding proteins, regulates muscle-specific splicing enhancer-dependent alternative splicing. The Journal of biological chemistry. 2004; 279:17756–17764. [PubMed: 14761971]

Lind D, Franken S, Kappler J, Jankowski J, Schilling K. Characterization of the neuronal marker NeuN as a multiply phosphorylated antigen with discrete subcellular localization. Journal of neuroscience research. 2005; 79:295–302. [PubMed: 15605376]

Maloney SE, Rieger MA, Dougherty JD. Identifying essential cell types and circuits in autism spectrum disorders. International review of neurobiology. 2013; 113:61–96. [PubMed: 24290383]

May PJ, Reiner AJ, Ryabinin AE. Comparison of the distributions of urocortin-containing and cholinergic neurons in the perioculomotor midbrain of the cat and macaque. The Journal of comparative neurology. 2008; 507:1300–1316. [PubMed: 18186029]

McDougle CJ, Naylor ST, Goodman WK, Volkmar FR, Cohen DJ, Price LH. Acute tryptophan depletion in autistic disorder: a controlled case study. Biol Psychiatry. 1993; 33:547–550. [PubMed: 8513041]

Mosienko V, Bert B, Beis D, Matthes S, Fink H, Bader M, Alenina N. Exaggerated aggression and decreased anxiety in mice deficient in brain serotonin. Translational psychiatry. 2012; 2:e122. [PubMed: 22832966]

Puelles, L.; Martinez-de-la-Torre, M.; Ferran, J-L.; Watson, C. Diencephalon. In: Watson, C.; Paxinos, G.; Puelles, L., editors. The Mouse Nervous System. London, UK: Academic Press; 2012.

Sears LL, Vest C, Mohamed S, Bailey J, Ranson BJ, Piven J. An MRI study of the basal ganglia in autism. Progress in neuro-psychopharmacology & biological psychiatry. 1999; 23:613–624. [PubMed: 10390720]

Tupal S, Rieger MA, Ling GY, Park TJ, Dougherty JD, Goodchild AK, Gray PA. Testing the role of preBotzinger Complex somatostatin neurons in respiratory and vocal behaviors. The European journal of neuroscience. 2014

Underwood JG, Boutz PL, Dougherty JD, Stoilov P, Black DL. Homologues of the Caenorhabditis elegans Fox-1 protein are neuronal splicing regulators in mammals. Molecular and cellular biology. 2005; 25:10005–10016. [PubMed: 16260614]

Wagnon JL, et al. CELF4 regulates translation and local abundance of a vast set of mRNAs, including genes associated with regulation of synaptic function. PLoS genetics. 2012; 8:e1003067. [PubMed: 23209433]

Watson, C. Hindbrain. In: Watson, C.; Paxinos, G.; Puelles, L., editors. The Mouse Nervous System. London, UK: Academic Press; 2012a.

Watson, C. Motor nuclei of the cranial nerves. In: Watson, C.; Paxinos, G.; Puelles, L., editors. The Mouse Nervous System. London, UK: Academic Press; 2012b.

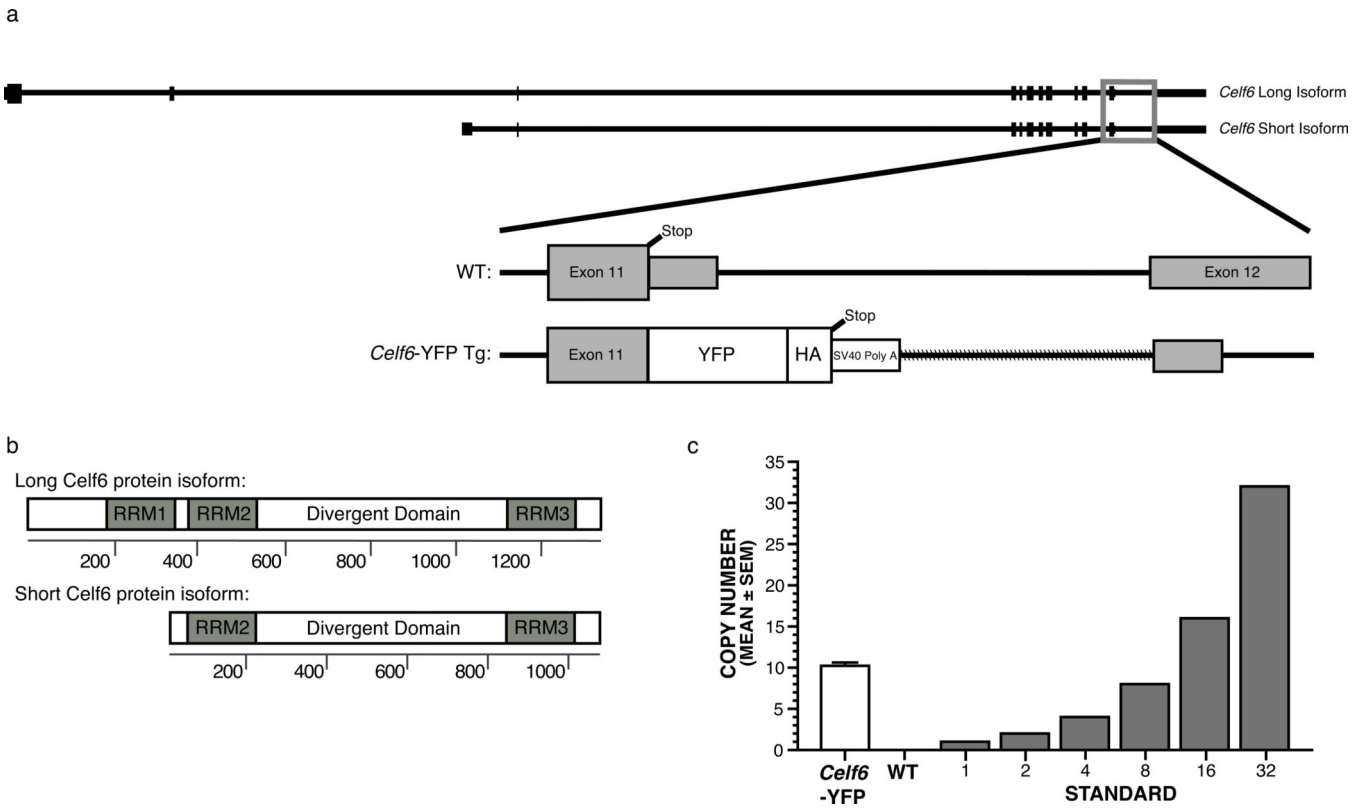

Fig. 1. Generation of a *Celf6* YFP BAC transgenic

a An illustration of the UCSC genome browser view of the *Celf6* gene in the mouse, showing 2 isoforms with 12 and 9 exons (black boxes), respectively, and a magnification of the modification made to the *Celf6*-YFP BAC transgene (Tg) targeted to the C-terminus (gray box outline) of the protein in Exon 11. The modification was inserted using a shuttle vector represented as backslashes, and contained the YFP protein with an HA tag in frame followed by a SV40 Poly A tail signal. **b** Both the long and the short isoform of the endogenous Celf6 protein share the C-terminus while containing alternative N-termini. The long Celf6 isoform houses 3 RNA recognition motifs (RRM) and the 268 amino acid divergent domain of unknown function. The short Celf6 isoform is lacking the RRM1 in the N-terminus. Both would be tagged at the C-terminus in the transgenic. **c** qPCR of genomic DNA compared to copy number standards revealed the *Celf6*-YFP mice contain an estimated 10 copies of the BAC integrated into the genome

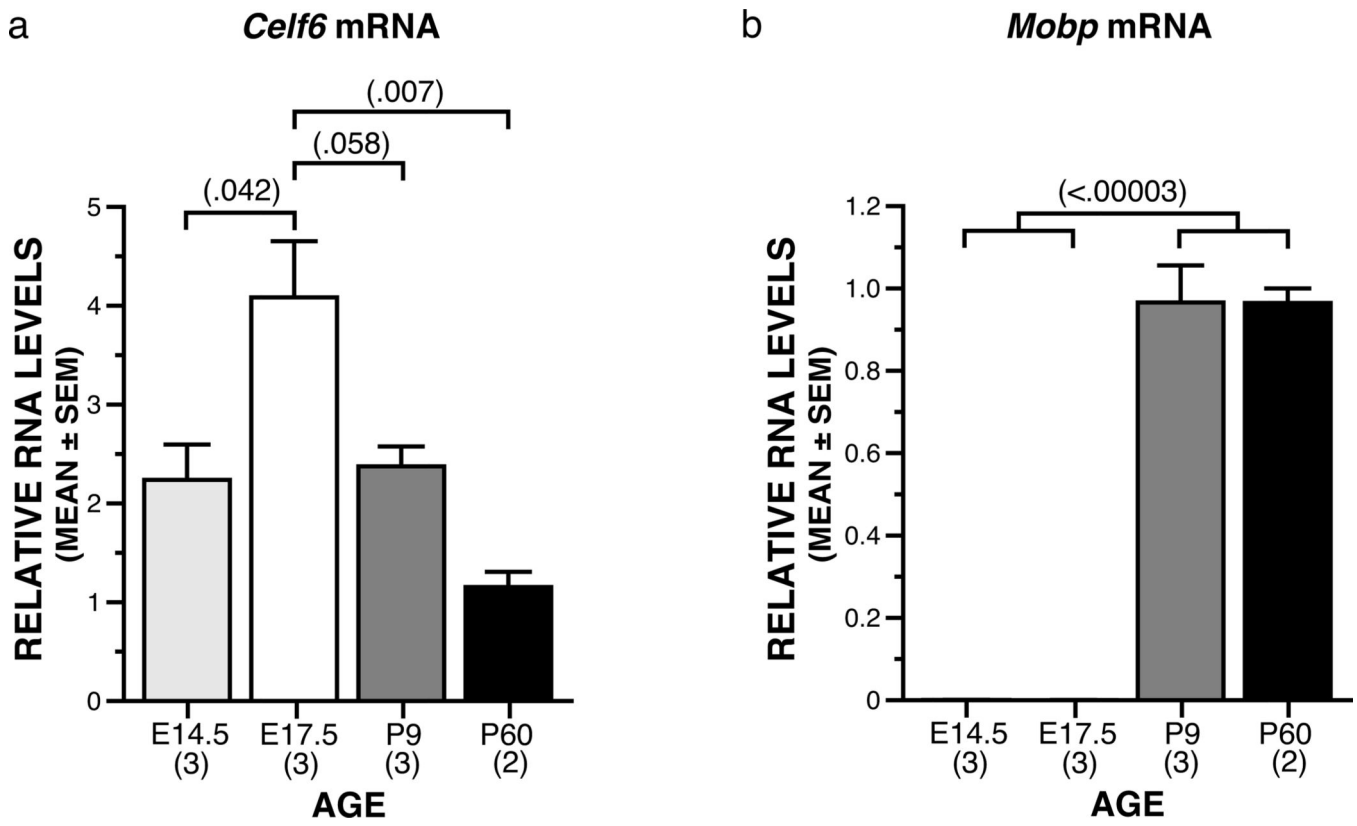

Fig. 2. Relative *Celf6* mRNA levels across neural development

Mean relative RNA levels across at E14, E17, P9 and P60 (mean ± SEM; n=3, 3, 3 and 2, respectively) of *Celf6* and *Mobp* from a triplicate RT-qPCR experiment following analysis by the ΔΔCT method and normalization to the endogenous control gene *Gapdh*. Levels are depicted relative to a P60 adult. **a** Transcript levels of *Celf6, F*(3,7) = 8.813, $p = .009$, are most abundant at E17.5, with a 1.8-fold increase from E14.5, a marginally significant 1.7-fold decrease in Celf6 mRNA was observed by P9 and a 3.5-fold decrease by P60. **b** As expected, transcripts of the myelination marker *Mobp* are exclusively expressed postnatally, $F(3,7) = 115.794$, $p = .000003$

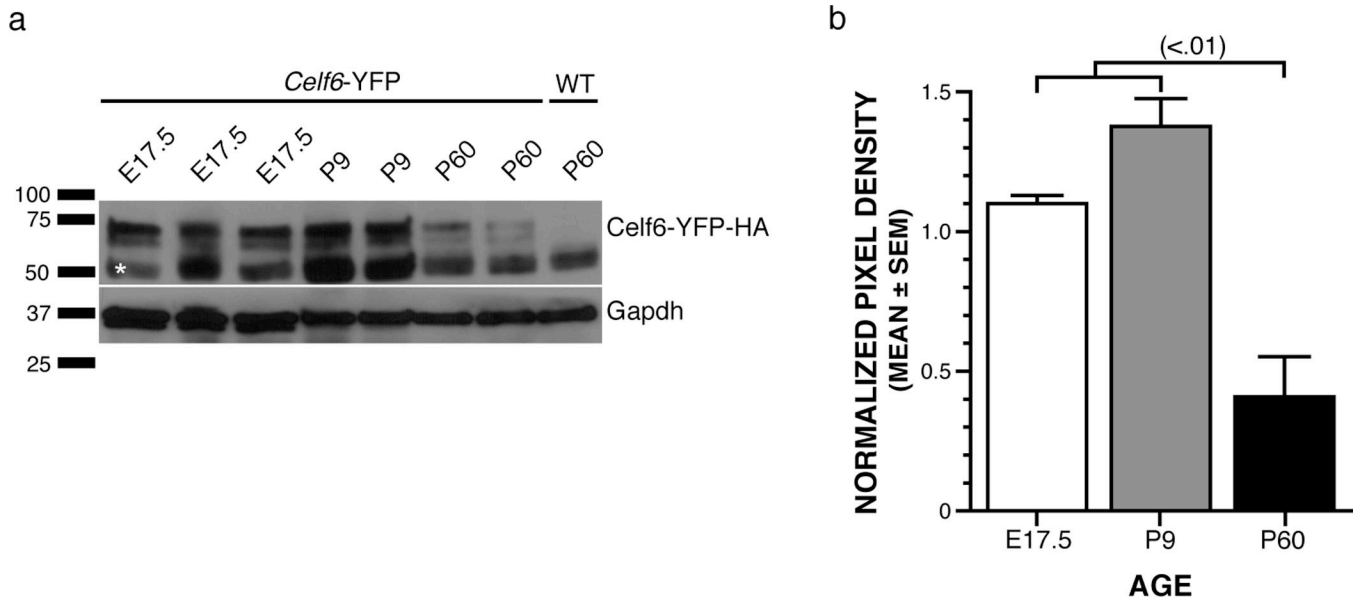

Fig. 3. Relative Celf6 protein levels across neural development

a Anti-HA immunoblot showing bands of 75 and 63 kDa, only in the *Celf6*-YFP samples, consistent with the predicted size of the YFP-HA tagged long and short isoforms. Asterisk: non-specific band (50 kd) present in both *Celf6*-YFP and WT samples. **b** Levels at E17, P9 and P60 (mean ± SEM; n=3, 2 and 2, respectively) of Celf6 protein as determined by densitometric analysis across ages of Celf6-YFP-HA band pixel density normalized to the pixel density of the within-sample Gapdh band. Celf6 protein is present at greater abundance during both E17.5 and P9 then adult, $F(2,4) = 30.495$, $p = .004$, post hocs for both E17.5 and P9 vs. P60 ($p < .01$)

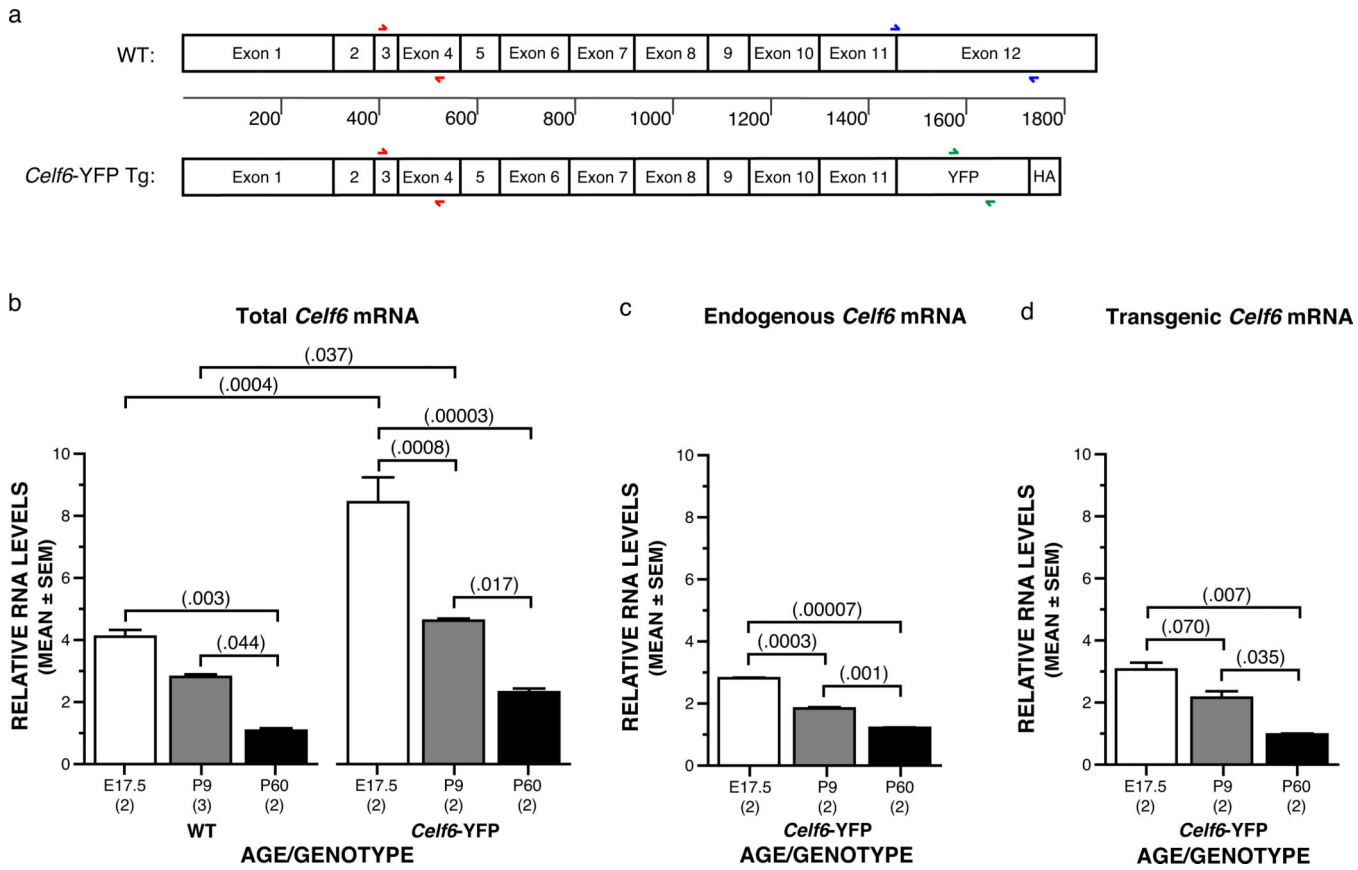

Fig. 4. The presence of the*Celf6*-YFP transgene does not influence the endogenous age-dependent patterns of *Celf6* mRNA transcription

RT-qPCR data analyses revealed endogenous and transgenic *Celf6* mRNA levels exhibit a parallel decrease across development. **a** An illustration of the WT and *Celf6*-YFP transgenic (Tg) cDNA regions amplified by the 3 primer sets used in B (red), C (blue) and D (green). **b** Relative mRNA levels amplified regardless of genetic origin (endogenous gene vs. transgene). The age-dependent pattern, E17.5 > P9 > P60, observed in tissue from WT brains (left; $F(2,7) = 21.826$, $p = .011$) is mirrored in tissue from Celf6-YFP transgenic brains (right; $F(2,7) = 90.203$, $p = .0001$). However, more total *Celf6* mRNA was present in the *Celf6*-YFP transgenic brain tissue overall, $F(1,7) = 90.856$, $p = .00003$, and at ages E17.5 and P9, $F(1,7) = 88.556$, $p = .0004$ and $F(1,7) = 18.655$, $p = .037$, respectively. **c** The relative mRNA amplified from only the endogenous Celf6 gene revealed the WT-like age-dependent patterns in brain tissue extracted from Celf6-YFP transgenic mice, $F(2,3) = 842.686$, $p = .00008$. **d** The relative mRNA amplified from only the transgene revealed the endogenous-like age-dependent patterns in brain tissue extracted from Celf6-YFP transgenic mice, $F(2,3) = 35.788$, $p = .008$. *All bars mean ± SEM*

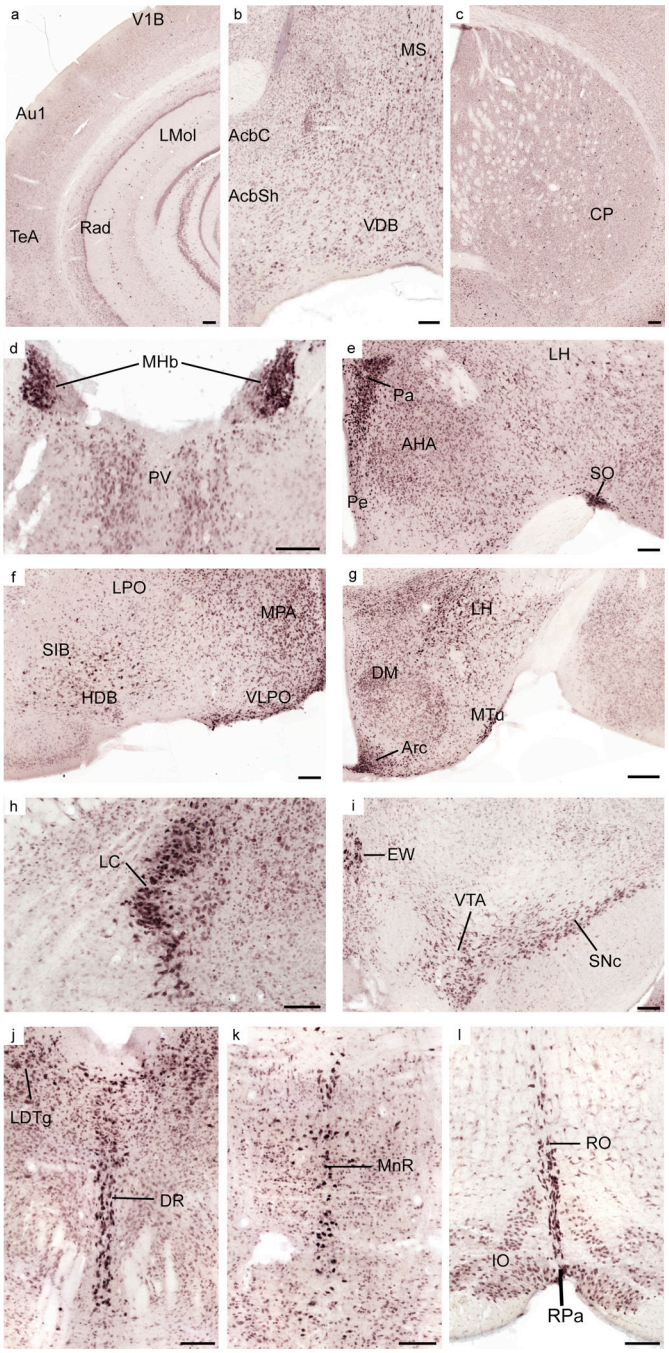

Fig. 5. Scattered expression of Celf6 protein was observed throughout the C57BL/6J adult mouse brain with select regions of high expression

Immunohistochemistry revealed Celf6 protein expression varied across the adult mouse brain with highest expression in the diencephalon and neuromodulatory populations of the midbrain and hindbrain. **a** Scattered cells displayed the greatest intensity of Celf6 protein in the isocortex and the hippocampus, with light expression in cells of the Rad and LMol layers across Fields CA1-3. **b–c** Within the subpallial structures, the highest expression was observed in the regions comprising the basal forebrain, including the MS and VDB. The

striatum, CP and Acb, contained scattered cells with moderate Celf6 protein signal. **d** Very high expression was observed in the MHb and moderate expression in the PV. **e–g** Many nuclei of the hypothalamus showed expression of Celf6 protein, with the greatest expression in nuclei adjacent to the ventral portion of the third ventricle. **h** The highest overall expression in the midbrain and hindbrain areas was observed in the LC. **i** High expression was also observed in the EW and moderate expression in the VTA and SNc. **j–l** The raphe nuclei contained high expression of Celf6 protein, including the DR, MnR, RO, and RPa. Moderate expression was observed in adjacent areas including the LDTg and IO. *For abbreviations, see list. Scale bars all* 125 μm

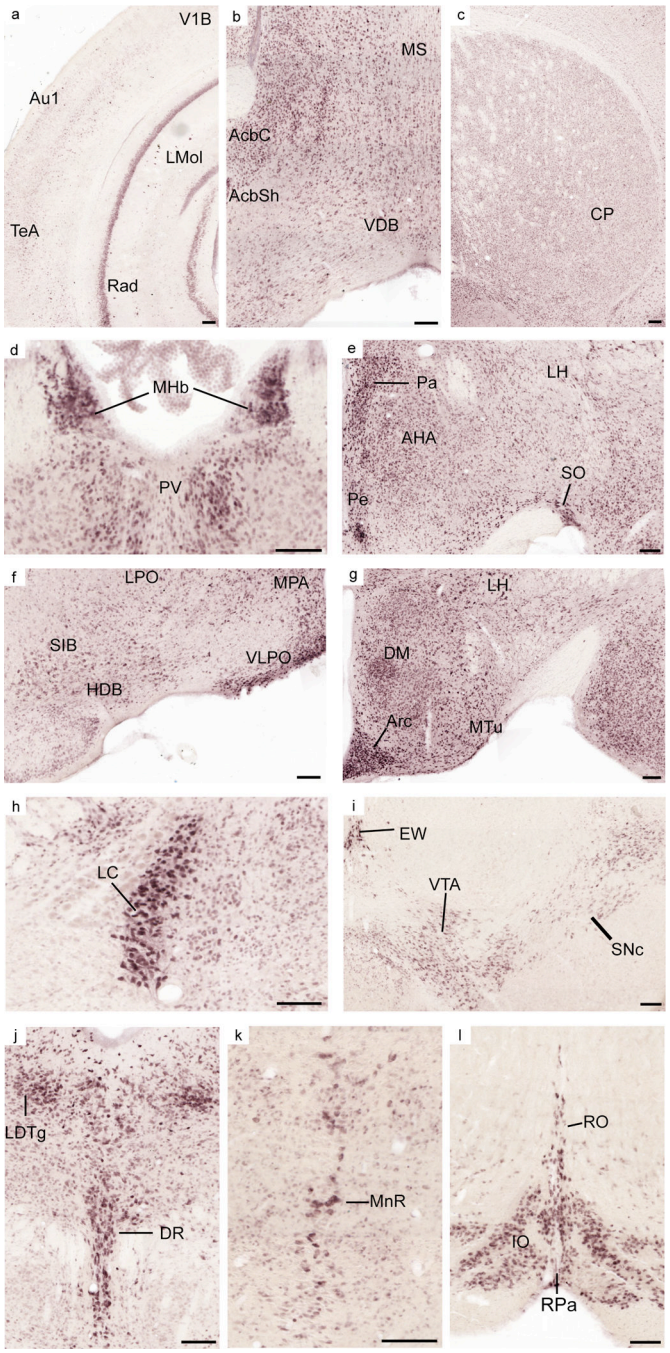

Fig. 6. Analysis of *Celf6*-YFP gene expression replicates observations with Celf6 antibody

Immunohistochemistry for YFP revealed comparable spatial expression between YFP localization in transgenic mice and Celf6 polyclonal antibody in WT mice. **a–l** All regions same as Fig. 5. *For abbreviations, see list. Scale bars all* 125 μm

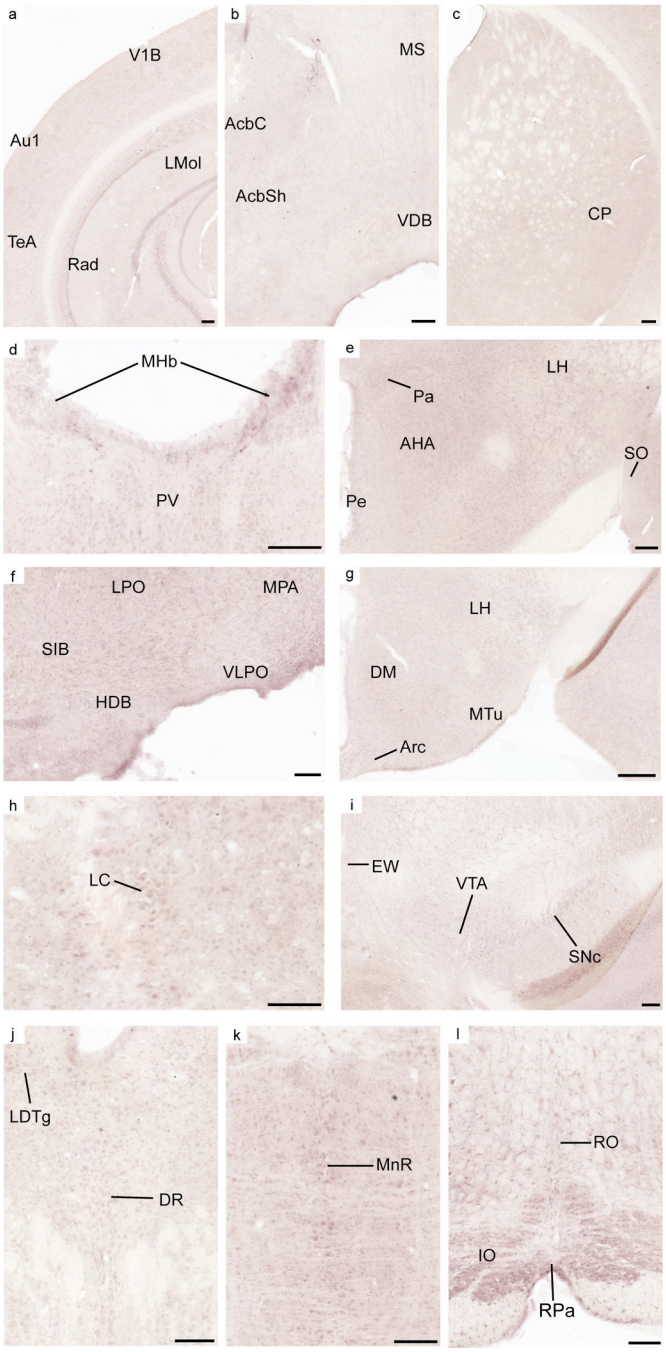

Fig. 7. Celf6 polyclonal antibody shows no specific signal in Celf6 knockout brain

Immunohistochemistry with anti-Celf6 revealed no specific cellular labeling in the adult mouse brain null for Celf6. Experiment conducted in parallel with WT mouse tissue (Fig. 5). **a–l** All regions same as Fig. 5. *For abbreviations, see list. Scale bars all* 125 μm

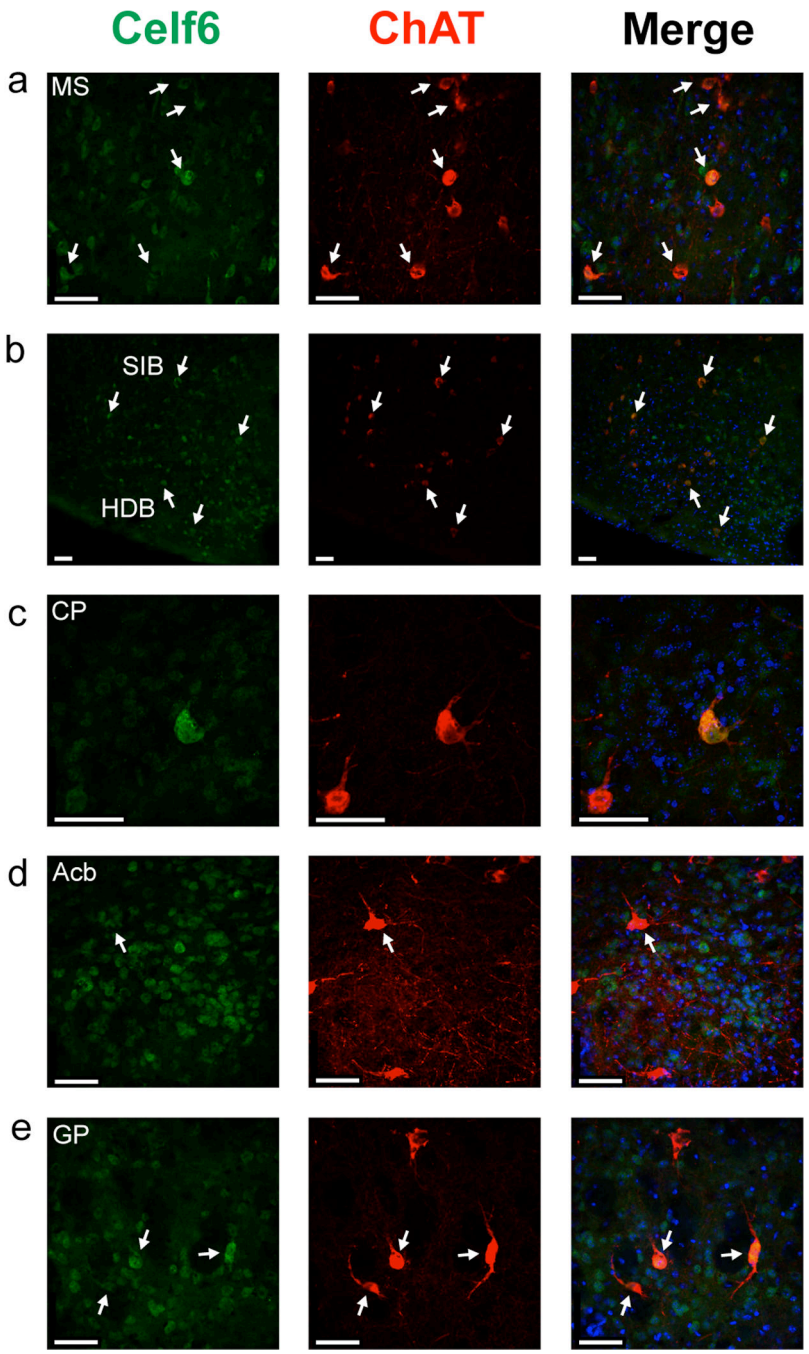

Fig. 8. Colocalization of Celf6 within cholinergic cells of the forebrain

Double-labeling confocal immunofluorescence images demonstrated Celf6 protein localization within cells expressing ChAT, in the forebrain. **a–b** Within the basal forebrain, Celf6 was observed in the cholinergic cells of the MS, HDB, and SIB. **c–e** Celf6 also was observed in the cholinergic neurons of the CP, Acb, and GP. *White arrows indicate examples of colocalization. For abbreviations, see list. Scale bars all* 51.00 μm

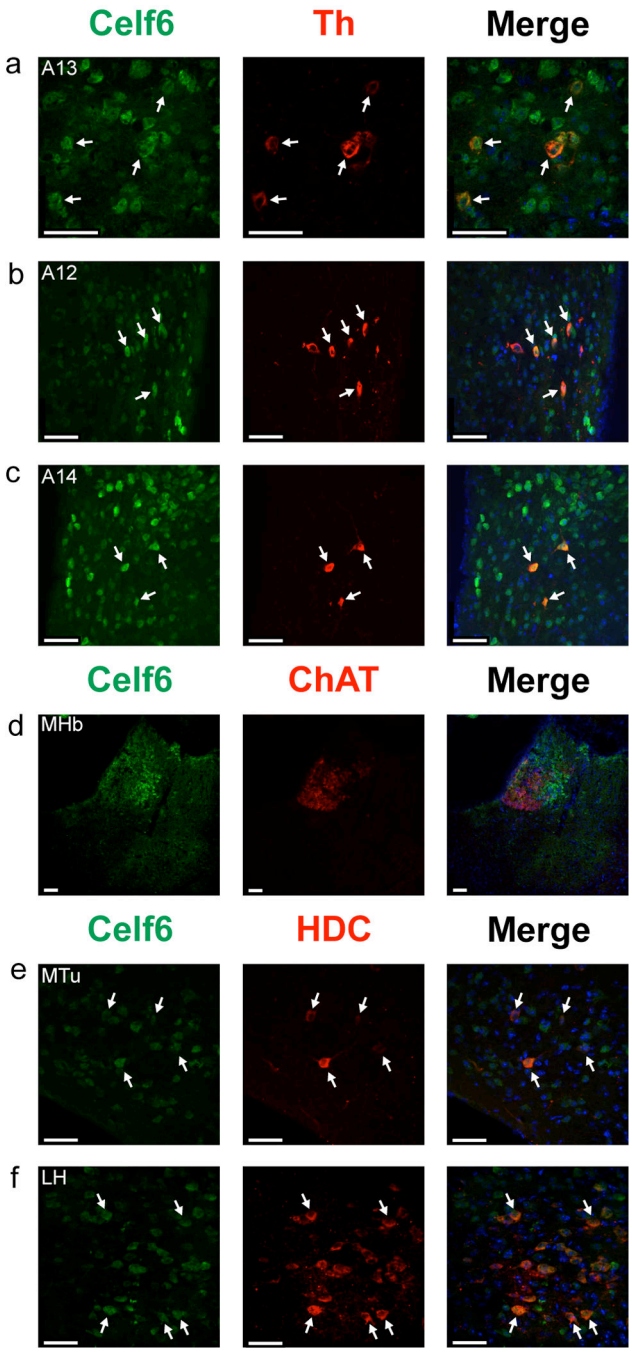

Fig. 9. Colocalization of Celf6 with neuromodulatory populations of the diencephalon

Double-labeling confocal immunofluorescence images demonstrated Celf6 protein colocalization with neuromodulatory populations of the diencephalon. **a–c** Celf6 antibody colocalized with Th, in the A13, A12, and A14 dopamine cell populations. **d** Within the MHb, Celf6 was found outside of the densely-packed populations of cholinergic cells labeled with ChAT. **e–f** Celf6 antibody also labeled the HDC-positive histaminergic cells of MTu and LH of the hypothalamus. *White arrows indicate examples of colocalization. For abbreviations, see list. Scale bars all* 51.00 μm

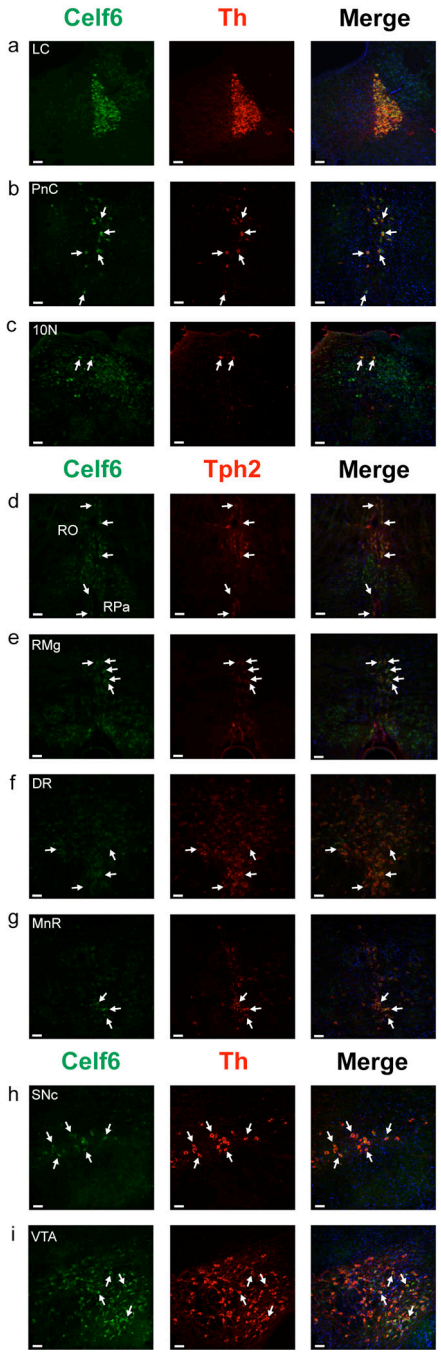

Fig. 10. Colocalization of Celf6 with neuromodulatory populations of the midbrain and hindbrain

Double-labeling confocal immunofluorescence images demonstrated Celf6 protein colocalization with neuromodulatory populations of the midbrain and hindbrain. **a–c** Celf6 antibody colocalized with Th in the noradrenergic cells of the LC, PnC, and 10N. **d–g** Celf6 antibody colocalized with serotonergic cells labeled with Tph2 in all of the raphe nuclei, including the RPa, RO, RMg, DR, MnR. **h–i** Celf6 antibody colocalized with Th in the large A9 and A10 dopamine cell populations, also known as the SNc and VTA, respectively.

White arrows indicate examples of colocalization. For abbreviations, see list. Scale bars all 51.00 μm

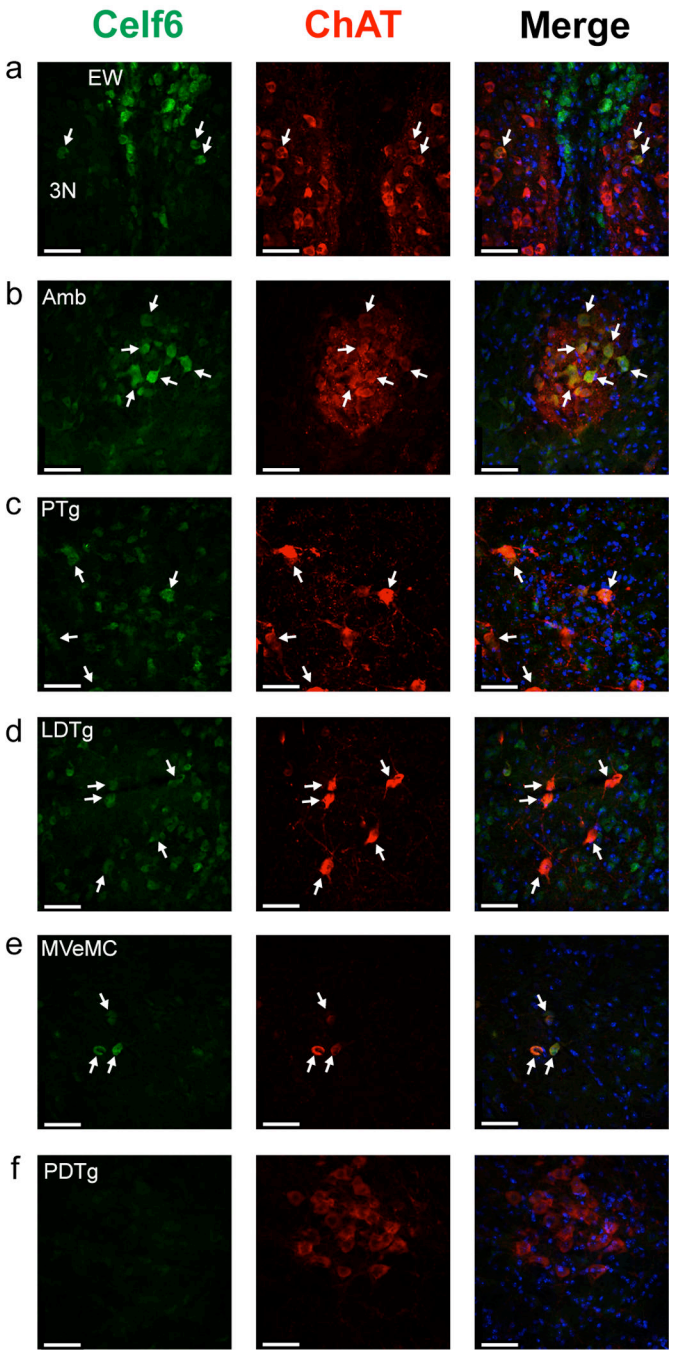

Fig. 11. Colocalization of Celf6 with cholinergic populations of the hindbrain

Double-labeling confocal immunofluorescence images demonstrating Celf6 protein colocalization with a subset of populations of cholinergic (ChAT+) cells of the hindbrain. **a–b** Celf6 was not observed in the cholinergic preganglionic cells of EW, and overlapped with only a few of the cholinergic motor neurons of 3N but with many of the motor neurons of Amb. **c–e** Celf6 was present in at least a portion of the cholinergic cells of the PTg, LDTg, and MVeMC. **f** Celf6 was absent from the PDTg. *White arrows indicate examples of colocalization. For abbreviations, see list. Scale bars all* 51.00 μm

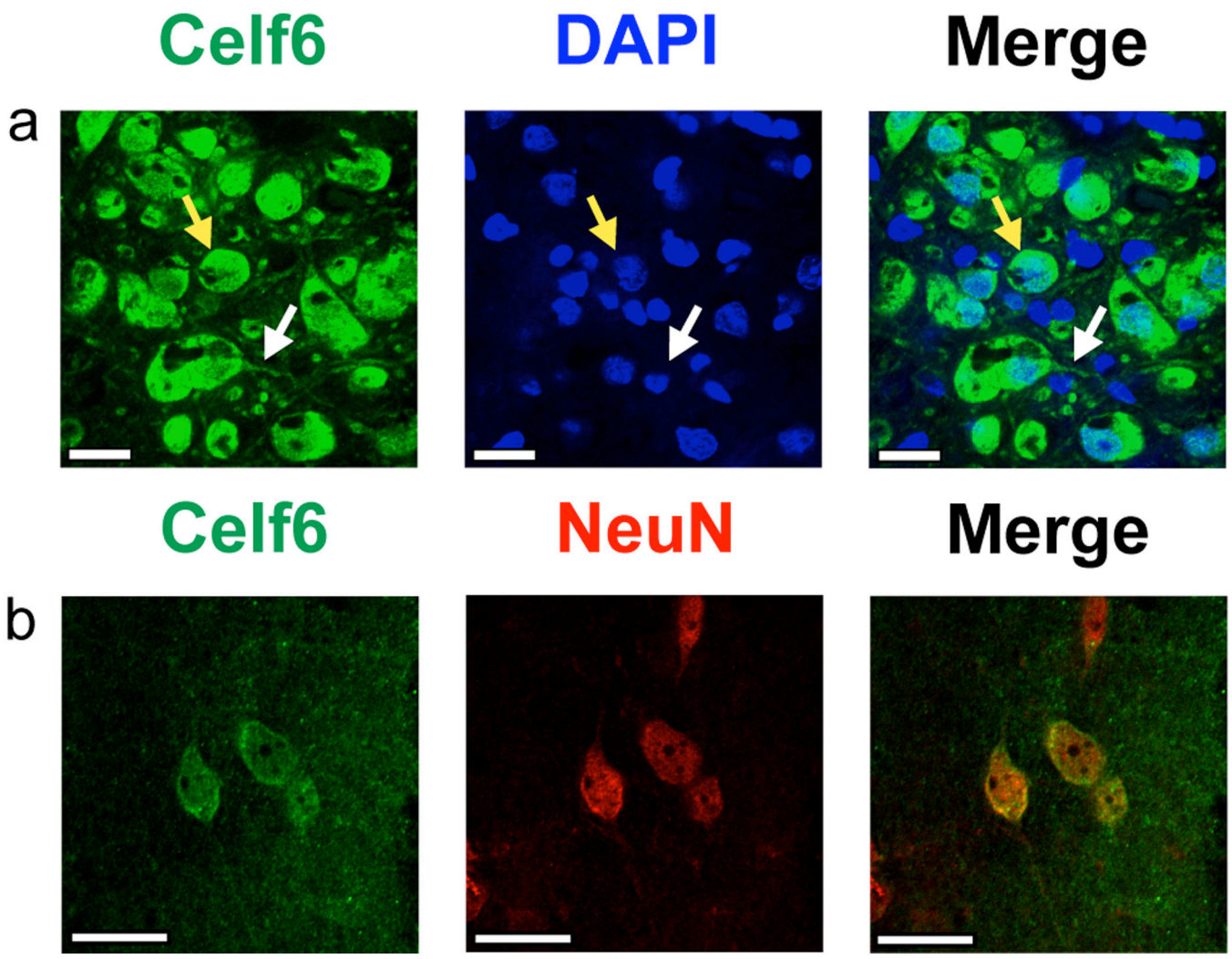

Fig. 12. Subcellular localization of Celf6 protein

High-magnification confocal immunofluorescence microscopic images demonstrate Celf6 protein subcellular localization. **a** Celf6 antibody labeled both the nucleus, as seen by overlap with the nuclear marker DAPI (an example indicated by the yellow arrows), and the surrounding cytoplasm. Dim Celf6 labeling was also observed in the neurites, indicated by the white arrows. Images of LC. **b** Complete overlap was observed between Celf6 antibody and NeuN (Rbfox3) antibody. NeuN has a known role as a splicing factor but is localized to both the cytoplasm and nucleus. Images of Hypothalamus. *For abbreviations, see list. Scale bars all* 20.00 μm

Table 1

Primer Sequences

Oligo sequences used to amplify gene products in for genotyping offspring of *Celf6*-YFP x C57BL/6J (WT) breeding crosses and RT-qPCR analysis of *Celf6* mRNA levels, endogenous and transgenic, across different ages.

RT-qPCR Primers

Gene	Primer	Sequence
HA-tagged YFP (DNA)	F	TTAAGCGTAGTCTGGGACGTCGTATGGGT
	R	CTACGTCCAGGAGCGCACCATCTTCTT
Celf6 (Exons 3 and 4)	F	ATCGTCCGATCCAAGTGAAGC
	R	CTCCTCGATATGGCCGAAGG
Mobp	F	AACTCCAAGCGTGAGATCGT
	R	CAGAGGCTGTCCATTCACAA
Gapdh	F	AGGTCGGTGTGAACGGATTTG
	R	GGGGTCGTTGATGGCAACA
Celf6 WT (Exon 12)	F	ACTGACCAGTCACAGACAGAAACTGAAGAAT
	R	GCCTCTCCAGCATTTCTGTGCTTTTCTGTT
YFP (cDNA)	F	AGGAGCGCACCATCTTCTTC
	R	CCGTCCTCCTTGAAGTCGATG

Table 2

Primary antibodies

Primary antibodies employed to determine regional and cell-type specific Celf6 protein expression in the WT and *Celf6*-YFP transgenic brains.

Primary Antibodies

Antibody	Dilution/species	Source and item no.
Celf6	1:250-10:000, rabbit polyclonal	Custom (Dougherty et al., 2013), NA
Tyrosine hydroxylase (Th)	1:500, mouse monoclonal	Millipore, MAB318
Tryptophan hydroxylase 2 (Tph2)	1:1000, mouse monoclonal	Millipore, MAB5278
Choline acetyltransferase (ChAT)	1:100, goat polyclonal	Millipore, AB144P
Yellow fluorescent protein (YFP)	1:1000-5000, chicken polyclonal	Aves Labs Inc, GFP-1020
Histidine decarboxylase (HDC)	1:1000, rabbit polyclonal	Boster Biological Technology LT, PA1703

Table 3

Relative density and intensity of Celf6 expression in the adult C57BL/6J mouse brain

Expression density level of Celf6 is indicated by + (scattered cells), ++ (light density), +++ (moderate density), or ++++ (high density). Signal intensity of Celf6 is indicated by + (light signal), ++ (moderate signal), or +++ (high signal). The overall expression score for each region was calculated by multiplying density level by signal intensity. Thus, the expression scores indicate the following: 1 – 2, light expression; 3 – 6, moderate expression; 8 – 9, high expression; and 12, very high expression.

GLOBAL REGION Specific Region	Density	Intensity	Overall Expression
ISOCORTEX			
Anterior olfactory area	+	+++	**3**
Agranular insular	+	++	**2**
Cingulate	+	++	**2**
Dorsal peduncular	++	++	**4**
Dysgranular insular	+	++	**2**
Granular insular	+	++	**2**
Infralimbic	++	++	**4**
Medial orbital	++	+	**2**
Parietal association	++	++	**4**
Piriform, polymorph layer	+	++	**2**
Piriform, pyramidal layer	+++	++	**6**
Prelimbic	++	++	**4**
Primary motor	+	++	**2**
Primary & secondary auditory	+	+	**1**
Primary & secondary somatosensory	+	++	**2**
Primary & secondary visual	++	+	**2**
Secondary motor	++	++	**4**
Tenia tecta	+	++	**2**
PARAHIPPOCAMPAL REGION			
Perirhinal	+	+	**1**
Ectorhinal	+	+	**1**
Entorhinal	++	+	**2**
HIPPOCAMPAL FORMATION			
Dentate gyrus, granular cell layer	++++	+	**4**
Dentate gyrus, polymorph layer	++	++	**2**
Hippocampus, lacunosum moleculare	++	+	**2**
Hippocampus, radiatum layer	+	++	**2**
Hippocampus, oriens layer	+	+	**2**
Hippocampus, pyramidal cell layer	++++	+	**4**
Subiculum	++	++	**4**
AMYGDALAR CORTEX AND NUCLEI			
Basolateral amygdaloid nucleus	+	++	**2**
Lateral amygdaloid nucleus	+	++	**2**

GLOBAL REGION Specific Region	Density	Intensity	Overall Expression
Medial amygdaloid nucleus	++++	+	**4**
SUBPALLIAL STRUCTURES			
Bed nuclei of the stria terminalis, anterior division	++++	++	**8**
Bed nuclei of the stria terminalis, posterior division	++++	+	**4**
Caudoputamen	+	++	**2**
Diagonal band nucleus	+++	++	**6**
Globus pallidus, external segment	+	++	**2**
Globus pallidus, internal segment	++	++	**4**
Lateral accumbens shell	+	+	**1**
Lateral septal nucleus, ventral part	+++	+	**3**
Medial septal nucleus	+++	+	**3**
Nucleus accumbens shell	+	+	**1**
Nucleus of the horizontal limb of the diagonal band	++	++	**4**
Nucleus of the vertical limb of the diagonal band	++	++	**4**
Substantia innominata	++	++	**4**
THALAMUS			
Central medial nucleus	+++	+	**3**
Medial geniculate complex	+++	+	**3**
Paraventricular nucleus	+++	+	**3**
Peripeduncular nucleus	+++	++	**6**
Subparafascicular nucleus, parvicellular part	+++	++	**6**
EPITHALAMUS			
Lateral habenula, dorsal aspect	+++	+++	**9**
Medial habenula, lateral aspect	++++	+++	**12**
Medial habenula, dorsal aspect	++++	+++	**12**
HYPOTHALAMUS			
Anterior hypothalamic nucleus	+++	+	**3**
Anterodorsal preoptic nucleus	++++	++	**8**
Anteroventral periventricular area	++++	++	**8**
Anteroventral periventricular nucleus	++++	++	**8**
Anteroventral preoptic nucleus	++	++	**4**
Arcuate hypothalamic nucleus (A12)	++++	+++	**12**
Dorsomedial nucleus of the hypothalamus	++	++	**4**
Dorsal premammillary nucleus	+++	++	**6**
Lateral hypothalamic area	++	++	**4**
Lateral preoptic area	++	++	**4**
Medial preoptic area	+++	++	**6**
Medial preoptic nucleus	++++	++	**8**
Medial tuberal nucleus, ventral and lateral aspect	+++	+++	**9**
Median preoptic nucleus	++++	++	**8**
Parastrial nucleus	+++	++	**6**

GLOBAL REGION Specific Region	Density	Intensity	Overall Expression
Paraventricular hypothalamic nucleus	++++	+++	**12**
Periventricular hypothalamic nucleus, preoptic part (A14)	++++	+++	**12**
Periventricular hypothalamic nucleus, posterior part (A12)	++++	+++	**12**
Periventricular hypothamalic nucleus, intermediate part	++	+++	**6**
Posterior hypothalamic nucleus	+++	++	**6**
Retrochiasmatic area, lateral & ventral aspect	++	++	**4**
Subthalamic nucleus	+++	++	**6**
Subparaventricular zone	++	+	**2**
Suprachiasmatic nucleus	++++	++	**8**
Retromammillary area	+	+++	**3**
Supraoptic nucleus	++++	+++	**12**
Tuberomammillary nucleus, dorsal part	+++	++	**6**
Ventral premammillary nucleus	++	++	**4**
Ventrolateral preoptic nucleus	+++	+++	**9**
Ventromedial hypothalamic nucleus	++++	+	**4**
PRETHALAMUS			
Zona incerta (A13)	+++	++	**6**
MIDBRAIN			
Caudal linear nucleus raphe (B8)	+++	++	**6**
Dorsal raphe nucleus (B6,7)	+++	+++	**9**
Pre-Edinger-Westphal nucleus	+++	+++	**9**
Edinger-Westphal nucleus	+++	+++	**9**
Interpeduncular nucleus	+	+++	**3**
Interpeduncular nucleus, ventral region	+++	+	**3**
Laterodorsal Tegmental nucleus	++	++	**4**
Midbrain reticular nucleus	++	++	**4**
Midbrain reticular nucleus, retrorubral area (A8)	+++	++	**6**
Magnocellular reticular nucleus	+	+++	**3**
Oculomotor nucleus	+	++	**2**
Pedunculopontine nucleus	++	++	**4**
Periaqueductal gray	+	+	**1**
Rostral linear nucleus	+++	++	**6**
Substantia nigra, pars compacta (A9)	+++	++	**6**
Ventral tegmental area (A10)	+++	++	**6**
HINDBRAIN			
Dorsal cochlear nucleus	+++	+	**3**
Gigantocellular reticular nucleus	+	+	**1**
Inferior colliculus, dorsal nucleus	+++	++	**6**
Inferior olivary complex	+++	++	**6**
Lateral reticular nucleus (A1)	++	+++	**6**

GLOBAL REGION Specific Region	Density	Intensity	Overall Expression
Locus ceoruleus (A6)	++++	+++	**12**
Medial vestibular nucleus	+	+	**1**
Median raphe nucleus (B5,8)	+++	+++	**9**
Nucleus ambiguus	++++	++	**8**
Nucleus of the lateral lemniscus, ventral part	++	++	**4**
Nucleus prepositus	++	+++	**6**
Nucleus raphe magnus (B3)	+++	+++	**9**
Nucleus raphe obscurus (B2,4)	+++	+++	**9**
Nucleus raphe pallidus (B1)	+++	+++	**9**
Nucleus raphe pontis (B9)	++	+++	**6**
Parabrachial nucleus, lateral division	++++	++	**8**
Parabigeminal nucleus	++	+	**2**
Paragigantocellular reticular nucleus, dorsal part	++	+	**2**
Paragigantocellular reticular nucleus, lateral part	+++	++	**6**
Parvicellular reticular nucleus	++	++	**4**
Pontine central gray	+++	+	**3**
Pontine reticular nucleus (A7)	++	++	**4**
Spinal nucleus of the trigeminal, interpolar part, ventral and medial aspect	++	++	**4**
Superior olivary complex (A5)	+++	++	**6**
Sublaterodorsal nucleus of the pons	++	+++	**6**